

https://dspace.org/

Evolution of postcanine complexity in Gomphodontia Therapsida Cynodontia

Christophe Hendrickx; Nestor Abdala; F Filippini; S Wills; Roger Benson ...

https://hdl.handle.net/10539/43098
WOS

Downloaded from a DSpace repository. https://dspace.org/

Check for updates

Received: 15 December 2023 | Revised: 3 January 2024 | Accepted: 5 January 2024

DOI: 10.1002/ar.25386

SPECIAL ISSUE ARTICLE

The Anatomical Record WILEY

Evolution of postcanine complexity in Gomphodontia (Therapsida: Cynodontia)

Christophe Hendrickx[1,2] | **Fernando Abdala**[1,2] | **Florencia S. Filippini**[3,4] | **Simon Wills**[5,6] | **Roger Benson**[2,7] | **Jonah N. Choiniere**[2]

[1]Unidad Ejecutora Lillo, CONICET-Fundación Miguel Lillo, San Miguel de Tucumán, Argentina

[2]Evolutionary Studies Institute, University of the Witwatersrand, Johannesburg, South Africa

[3]Laboratorio de Becarios, Museo Argentino de Ciencias Naturales "Bernardino Rivadavia", Buenos Aires, Argentina

[4]Consejo Nacional de Investigaciones Científicas y Técnicas (CONICET), Buenos Aires, Argentina

[5]Fossil Reptiles, Amphibians and Birds Section, Natural History Museum, London, UK

[6]Department of Earth & Planetary Sciences, Birkbeck College, London, UK

[7]Division of Paleontology, American Museum of Natural History, New York, New York, USA

Correspondence
Christophe Hendrickx, Unidad Ejecutora Lillo, CONICET-Fundación Miguel Lillo, Miguel Lillo 251, San Miguel de Tucumán 4000, Tucumán, Argentina.
Email: christophendrickx@gmail.com

Funding information
Agencia Nacional de Promoción Científica y Tecnológica, Grant/Award Numbers: 181417, PICT 2020–01498; PAST; Consejo Nacional de Investigaciones Científicas y Técnicas; NRF Competitive Support for Rated Researchers, Grant/Award Number: 98906; NRF African Origins Platform, Grant/Award Number: 98800; University Research Committee (URC) of the University of the Witwatersrand; DST-NRF Centre of Excellence, Palaeosciences, Grant/Award Numbers: PPD2015/17CH, CoE2017-038

Abstract

Gomphodonts form a Triassic radiation of small to medium-bodied (<0.5–2.5 m in length) quadrupedal cynodonts characterized by labiolingually expanded gomphodont postcanines. They were the dominant cynodont group in Middle and Late Triassic ecosystems from the Southern Hemisphere and the first predominantly herbivorous cynodonts to evolve. Gomphodonts were also the first therapsids to develop hypsodonty and a dentition with complex occlusal patterns, and their highly diagnostic upper and lower postcanines show many different morphologies. Here, we explored dental complexity in gomphodont cynodonts through time using geographic information system analysis and orientation patch count applied on 3D crown surfaces of upper and lower gomphodont postcanines belonging to 32 gomphodont taxa. This study reveals that the peak in postcanine complexity was reached early in the evolution of gomphodonts with the emergence in the Early Triassic of omnivorous or insectivorous forms with postcanines made of well-separated cusps and cingular cuspules. Traversodontids evolved simpler postcanines via coalescence of cusps into crests and the development of large occlusal basins, and the Middle Triassic radiation of traversodontids led to a sharp decrease in mean postcanine complexity. Simplification of the postcanines in traversodontids is interpreted as being related to a gradual increase in the consumption of plant material. Interestingly, the trend of insectivory/omnivory high postcanine complexity and herbivory low dental complexity in gomphodonts is opposite to the trend of dental complexity reported in some extant mammals, with omnivorous having low dental complexity and herbivorous higher. Postcanine complexity remained relatively stable throughout the evolution of traversodontids and only slightly diminished in the Late Triassic due to the presence of minute forms with particularly simple postcanines in the Rhaetian. The major phylogenetic diversity and taxonomic richness of Gomphodontia are represented in two periods of time: at the end of the Anisian, an age in which the postcanine complexity is simplifying, and at the early Carnian when the postcanine complexity in traversodontids, the only Gomphodontia represented, is stable.

KEYWORDS

Cynognathia, dental evolution, gomphodont, orientation patch count, teeth

 © 2024 American Association for Anatomy.

1 | INTRODUCTION

Vertebrate teeth are an excellent proxy to reconstruct palaeoecology because they are directly involved in feeding, and their morphology provides evidence of feeding strategy (Hillson, 2005; Schwenk, 2000). Living mammals are among the most morphologically diverse groups of tetrapods, filling a broad range of ecologies and displaying a wide variety of tooth morphologies (Ungar, 2010). Premammalian cynodonts include the closest evolutionary relatives of mammals and evolved teeth with complex occlusal surfaces in multiple groups independently from ancestors with more simple tooth morphologies (e.g., Abdala et al., 2006; Crompton, 1972; Crompton & Jenkins, 1968; Hendrickx et al., 2019, 2020; Hopson & Barghusen, 1986; Hopson & Kitching, 2001; Liu & Abdala, 2014; Sidor & Hopson, 2018; Ungar, 2010). Among these, Gomphodontia is a Triassic radiation of small-to-medium-bodied cynodonts (i.e., ~30–600 mm in maximum skull length; 1–2.7 kg of body weight in the small traversodontid *Andescynodon* and 100–150 kg in the large *Exaeretodon*; Filippini et al., 2022) known from all continents but Australia (Abdala et al., 2006; Hopson, 2014; Reisz & Sues, 2000; Figure 1a). Gomphodonts were one of the most diverse groups of cynodonts and one of the dominant groups of land vertebrates in the Middle to Late Triassic faunas of South America and southern Africa (Abdala et al., 2020; Abdala & Gaetano, 2018; Abdala & Ribeiro, 2003). Though the skull and body plan of gomphodonts was relatively conserved during the evolution of the group, the dentitions of these cynodonts are complex and morphologically diverse (Abdala & Ribeiro, 2003; Crompton, 1972; Hendrickx et al., 2019, 2020; Kemp, 2005; Liu & Sues, 2010; Martinelli, 2010; Figure 1). Gomphodont cynodonts are distinctly heterodont and bear conical, spatulated or subtriangular incisors, large pointed canines, and heterodont postcanines, mostly featuring labiolingually expanded teeth known as gomphodont postcanines (Figure 1a) but in some cases also simple mesial conical and distal sectorial postcanines (Crompton, 1972; Hendrickx et al., 2019). Gomphodont postcanines are the most common elements of the dentition of this lineage and show a large array of morphologies (e.g., Abdala et al., 2006; Crompton, 1972; Hendrickx et al., 2019, 2020; Hopson, 2014; Seeley, 1895, 1908). Gomphodonts are in fact among the earliest known cynodonts to develop a dentition with a precise occlusal pattern, the first radiation of herbivorous cynodonts to appear, and the earliest animals to evolve hypsodont postcanines (Crompton, 1972; Melo et al., 2019). They radiated into three main clades mostly differentiated on postcanine heterodonty and morphology, namely Diademodontidae, Trirachodontidae, and Traversodontidae (Abdala & Ribeiro, 2010; Crompton, 1972; Hendrickx et al., 2016, 2019; but see Hendrickx et al., 2020; Figure 2). Diademodontids postcanines are simple mesial conical teeth, ovoid gomphodont (Figure 1g), and distal sectorial postcanine teeth, whereas ellipsoid gomphodont (Figure 1k) and distal sectorial teeth are typical of trirachodontids (Hendrickx et al., 2019). The final group of this lineage (but see Hopson and Kitching (2001) and Sidor and Hopson (2018) for a different view), traversodontids, possesses rectangular to trapezoidal upper and quadrangular lower postcanine teeth often dug by deep occlusal basins (Figure 1i,m,o), with some limited cases of sectorial postcanines mainly in juvenile individuals (e.g., Crompton, 1972; Goñi & Goin, 1988; Hendrickx et al., 2020; Liu & Abdala, 2014; Liu & Sues, 2010).

Although the external morphology of gomphodont postcanines is relatively well-documented, a broad comparative survey of the evolution of tooth complexity through time remains to be done. Similar studies on mammals, such as disparity in dental complexity in multituberculates (Wilson et al., 2012), carnivorans, and rodents (Evans et al., 2007), have yielded surprising results (i.e., disparity in dental complexity directly reflects diet and correlates with taxonomic richness and disparity in body size). Morphological diversity and diversification in nonmammalian cynodonts were explored by Ruta et al. (2013) by assembling a data matrix after previous studies of several researchers (e.g., Abdala, 2007; Liu & Olsen, 2010) but these authors did not investigate dental complexity. Several recent contributions had modified our knowledge of the relationships of nonmammaliaform cynodonts and some of its subgroups (e.g., Abdala et al., 2019; Gaetano et al., 2022; Huttenlocker & Sidor, 2020; Kammerer, 2016; Martinelli et al., 2017; Velazco et al., 2017). In addition, a huge improvement was recently produced in the sampling of dental characters in gomphodont cynodonts (accompanied by a proposal of standardization of dental terminology) after the contributions of Hendrickx et al. (2019, 2020). This study, which represents a natural extension of those previous researches, aims to explore gomphodont postcanine complexity in gomphodont cynodonts through time with the goal of experimenting new avenues to interpret feeding aspects of this group and illuminating macroevolutionary processes that may represent the key to understand their richness and success throughout the Triassic.

1.1 | Institutional abbreviations

BP, Evolutionary Studies Institute, University of the Witwatersrand, Johannesburg, South Africa; BSP, Bayerische Staatssammlung für Paläontologie und Historische Geologie, Munich, Germany; CAMZM, University

19328494, 2024, 4, Downloaded from https://anatomypubs.onlinelibrary.wiley.com/doi/10.1002/ar.25386 by University Of Witwatersrand, Wiley Online Library on [07/11/2024]. See the Terms and Conditions (https://onlinelibrary.wiley.com/terms-and-conditions) on Wiley Online Library for rules of use; OA articles are governed by the applicable Creative Commons License

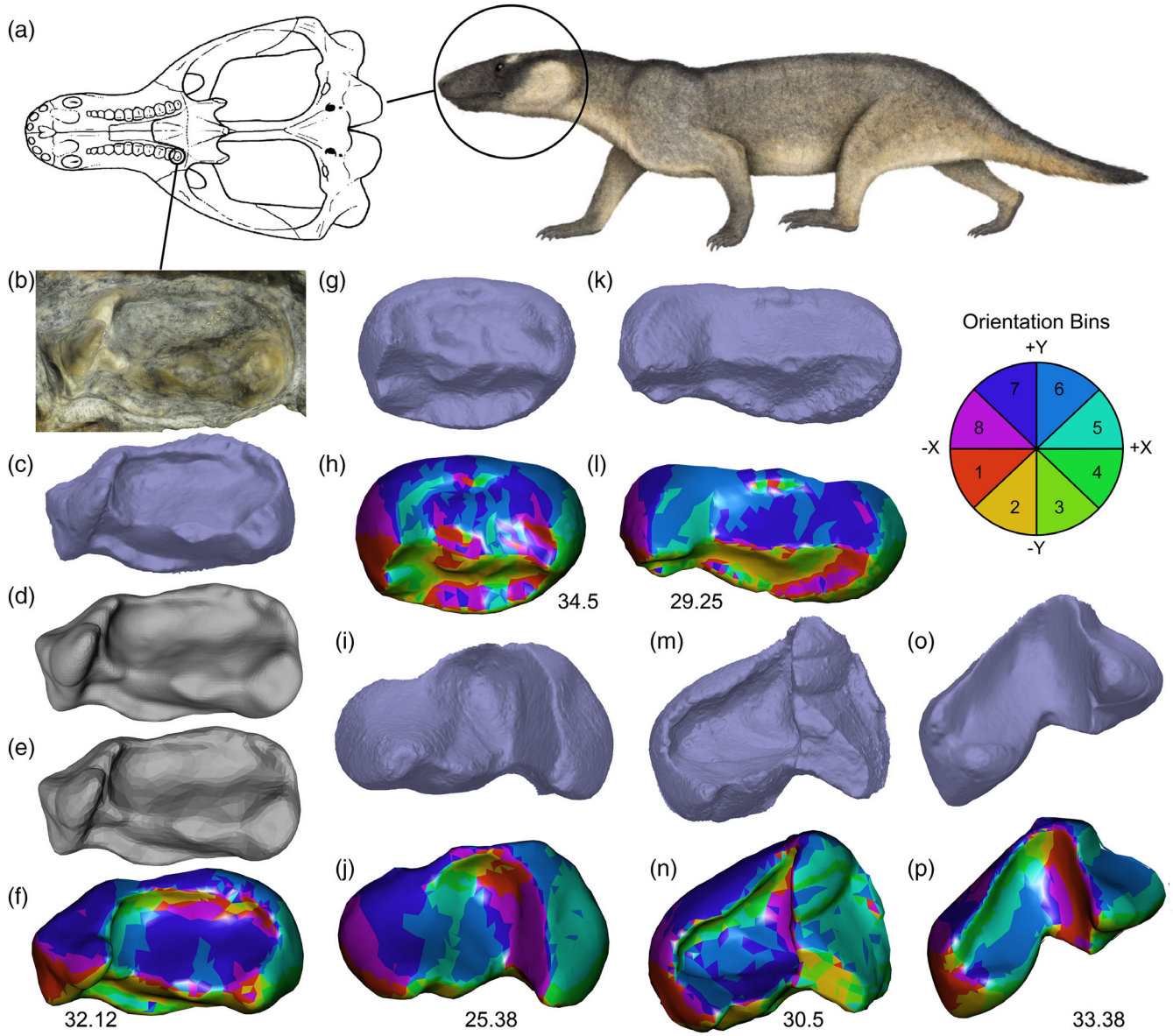


FIGURE 1 Method to explore dental complexity in gomphodont cynodonts. (a–f) Step-by-step process to calculate dental complexity in the last right upper postcanine of the traversodontid *Traversodon stahleckeri* (GPIT/RE/7170). (a) The best preserved postcanine, typically from the distalmost part from the jaw, of a gomphodont skull (here schematized with the cranium of the traversodontid *Pascualgnathus* in palatal view, modified from Martinelli, 2010) is selected and photographed with a camera or a portable microscope AM411T-Dino-Lite Pro (reconstruction of the traversodontid *Massetognathus* by Gabriel Ugueto; courtesy of Gabriel Ugueto; used with permission); (b) the tooth is reconstructed in 3D through photogrammetry using the software Agisoft Photoscan Standard Version 1.3.4; (c) the postcanine is isolated from the rest of the jaw using the free-form selection tool in Agisoft Photoscan; (d) the 3D model of the postcanine is then reconstructed and smoothen in MeshLab v.1.3.4.5027 BETA using the Poisson Surface Reconstruction tool; (e) the 3D model is decimated to 2000 faces using the R package MolaR; (f) postcanine complexity is finally calculated for the decimated 3D model in MolaR using the orientation patch count (OPC), which counts the number of patches in eight direction bins (with a minimum of 10 faces considered); (g–p) 3D-models, dental complexity (here illustrated with the number of patches of different colors), and OPC values in (g, h) the diademodontid *Diademodon tetragonus* (SAM 571); (i, j) the arctotraversodontine traversodontid *Boreogomphodon jeffersoni* (USNM 437632); (k, l) the trirachodontid *Trirachodon berryi* (SAM K171); (m, n) the massetognathine traversodontid *Santacruzodon hopsoni* (MCN 2770); and (o, p) the gomphodontosuchine traversodontid *Exaeretodon argentinus* (PVL 2458).

Museum of Zoology, Cambridge, UK; CAPPA/UFSM, Centro de Apoio à Pesquisa Paleontológica da Quarta Colônia/Universidade Federal de Santa Maria, São João do Polêsine, Brazil; CGP, Council for Geosciences, Pretoria, South Africa; FMNH, Field Museum of Natural History, Chicago, Illinois, USA; GPIT, Institut und Museum für Geologie und Paläontologie der Universität Tübingen, Tübingen, Germany; GSN, Geological Survey of Namibia, Windhoek, Namibia; IRSNB, Institut Royal des Sciences Naturelles de Belgique, Brussels, Belgium; IVPP, Institute

19328494, 2024, 4, Downloaded from https://anatomypubs.onlinelibrary.wiley.com/doi/10.1002/ar.25386 by University Of Witwatersrand, Wiley Online Library on [07/11/2024]. See the Terms and Conditions (https://onlinelibrary.wiley.com/terms-and-conditions) on Wiley Online Library for rules of use; OA articles are governed by the applicable Creative Commons License

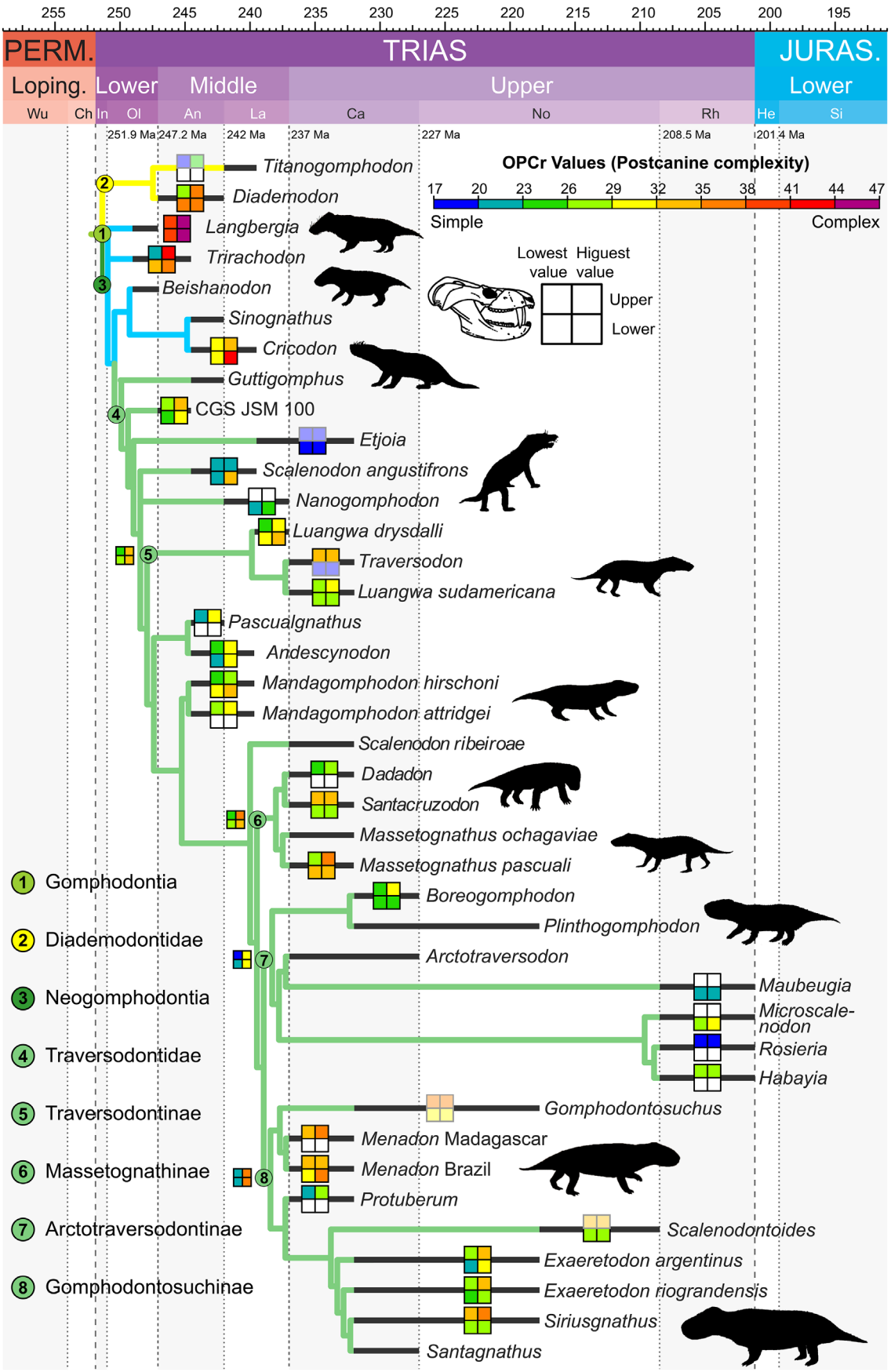


FIGURE 2 Legend on next page.

19328494, 2024, 4, Downloaded from https://anatomypubs.onlinelibrary.wiley.com/doi/10.1002/ar.25386 by University Of Witwatersrand, Wiley Online Library on [07/11/2024]. See the Terms and Conditions (https://onlinelibrary.wiley.com/terms-and-conditions) on Wiley Online Library for rules of use; OA articles are governed by the applicable Creative Commons License

for Vertebrate Paleontology and Paleoanthropology, Beijing, China; MACN-Pv, Museo Argentino de Ciencias Naturales "Bernardino Rivadavia", Buenos Aires, Argentina; MCN, Museu de Ciências Naturais do Rio Grande do Sul, Secretaria do Meio Ambiente e Infraestrutura, Porto Alegre, Rio Grande do Sul, Brazil; MCP, Laboratório de Paleontologia, Museu de Ciências e Tecnologia, Pontifícia Universidade Católica do Rio Grande do Sul, Porto Alegre, Rio Grande do Sul, Brazil; MNHN, Muséum National d'Histoire Naturelle, Paris, France; NHMUK, Natural History Museum, London, UK; NMQR, National Museum, Bloemfontein, South Africa; PVL, Colección Palaeontología de Vertebrados Lillo, Universidad Nacional de Tucumán, Argentina; SAM PK, Iziko, the South African Museum, Cape Town, South Africa; SMNS, Staatliches Museum für Naturkunde Stuttgart, Stuttgart, Germany; UA, Université d'Antananarivo, Antananarivo, Madagascar; UFRGS-PV, Setor de Paleovertebrados, Instituto de Geociências, Universidade Federal do Rio Grande do Sul, Porto Alegre, Rio Grande do Sul, Brazil; USNM, National Museum of Natural History, Washington DC, USA.

2 | MATERIALS AND METHODS

2.1 | Comparative anatomy, dental terminology and phylogeny

The postcanine dentition of early branching gomphodonts is strongly heterodont and made of conical, gomphodont, and sectorial teeth (e.g., *Diademodon*). Here, we explored dental complexity in Gomphodontia using exclusively gomphodont postcanines because (i) gomphodont teeth are the main dental component of the postcanine tooth row in the majority of gomphodont cynodonts (all non-diademodontid gomphodonts); (ii) most of gomphodonts do not have their postcanine dentition preserved entirely due to wear or taphonomical processes, making comparison of the whole postcanine complexity between gomphodont taxa unfeasible; and (iii) conical and sectorial postcanines are often incomplete and/or rarely fully prepared and, therefore, difficult to sample for dental complexity analyses. The gomphodont postcanines of 34 species-level gomphodont cynodonts deposited in 18 scientific collections from Argentina, Belgium, Brazil, China, France, Germany, Namibia, South Africa, the United Kingdom, and the United States of America were examined first-hand with the help of a digital camera Canon PowerShot SX60 HS and a portable microscope AM411T-Dino-Lite Pro (Table 1). CT-scan data on the dental material of the traversodontids *Luangwa drysdalli* (NHMUK R36995) and *Mandagomphodon attridgei* (NHMUK R8578) was additionally generated at the School of Earth Sciences X-ray Tomography Facility of the University of Bristol by one of us (RB) using X-Ray Computed Tomography (CT/microCT) Nikon Metrology XT H 225 ST with a voxel size of 0.028215 for *Luangwa* (1903 images) and 0.021226 for *Mandagomphodon* (1818 images).

The clade names and phylogenetic definitions compiled by Hendrickx et al. (2020) were used to discuss dental complexity in a phylogenetic context among Gomphodontia. The dental positional nomenclature follows Smith and Dodson (2003), whereas the anatomical nomenclature used to describe and annotate the external tooth morphology follows the terminology and abbreviations provided by Hendrickx et al. (2019). Dental complexity in gomphodonts was primarily visualized using the phylogenetic tree recovered by Hendrickx et al. (2020) and additionally examined using the alternative tree topologies recently obtained by Rayner et al. (2022) and Gaetano et al. (2022). Following Hendrickx et al. (2019, 2020), the Chinese taxa *Beishanodon youngi* (Gao et al., 2010) and *Sinognathus gracilis* (Young, 1959) were considered as gomphodonts, and the holotype and specimens referred to the species '*Cricodon kannameyeri*' by Sidor and Hopson (2018) were interpreted as younger individuals of *Trirachodon berryi*. Finally, the postcanine dentitions of the African and South American specimens of *Menadon besairiei* were considered separately to account for the dental variations observed by Hendrickx et al. (2020) between the holotype from Madagascar (Flynn et al., 2000; Kammerer et al., 2008) and the referred specimens from Brazil (Melo et al., 2015, 2019).

FIGURE 2 Phylogeny and postcanine complexity in gomphodont cynodonts throughout the Triassic. Dental complexity is visualized based on 10 increments of complexity ranging from 17 to 47, the OPCR values obtained from 3D models of postcanines decimated to 2000 faces with a minimum of 10 faces considered. The upper and lower squares of each square represent the complexity of the upper and lower postcanine teeth, respectively, whereas the left and right squares provide the lowest and highest values of dental complexity, respectively. Blurred/shaded squares (e.g., *Titanogomphodon*, *Etjoia*, *Traversodon*) illustrate dental complexity in particularly incomplete or worn-out postcanines. The smaller squares next to the traversodontid subclades (numbered 5–8) represent the ancestral condition of postcanine complexity in traversodontines, massetognathines, arctotraversodontines, and gomphodontosuchines. Black bar in each branch indicates temporal extension of the taxa. The phylogenetic tree follows the results of the cladistic analyses obtained by Hendrickx et al. (2020) and Schmitt et al. (2024). Black silhouettes credit: Gabriel Ugueto (*Cricodon*), Sergey Meleshin (*Scalenodon*), José Eduardo Camargo Martínez (all others). Skull of *Pascualgnathus* on the left of the square modified from Martinelli (2010).

19328494, 2024, 4, Downloaded from https://anatomypubs.onlinelibrary.wiley.com/doi/10.1002/ar.25386 by University Of Witwatersrand, Wiley Online Library on [07/11/2024]. See the Terms and Conditions (https://onlinelibrary.wiley.com/terms-and-conditions) on Wiley Online Library for rules of use; OA articles are governed by the applicable Creative Commons License

TABLE 1 List of the gomphodont cynodonts included in this study.

Taxa	Specimen	Included 3D-models
Andescynodon mendozensis	PVL 3894, 4390, 4907	Y
Boreogomphodon jeffersoni	USNM 437632, 448563	Y
Cricodon metabolus	CAMZM T905	Y
Dadadon isaloi	FMNH PR 2232	Y
Diademodon tetragonus	SAM PK K571	Y
Etjoia dentitransitus	GSN F1591	Y
Exaeretodon argentinus	MACN-Pv 18125; PVL 2458, 2467	Y
Exaeretodon riograndensis	MCP 1522 PV; UFRGS-PV 1096T	Y
Gomphodontosuchus brasiliensis	GPIT/RE/09397	N
Habayia halbardieri	IRSNB R203	Y
Langbergia modisei	NMQR 3251, 3255	Y
Luangwa drysdalli	BP/1/3731; NHMUK R36995	Y
Luangwa sudamericana	MCP 3167PV; UFRGS-PV 0267T	Y
Mandagomphodon attridgei	NHMUK R8578	Y
Mandagomphodon hirschsoni	NHMUK R8577	Y
Massetognathus ochagaviae	MCP 3871 PV	N
Massetognathus pascuali	BP/1/4245; PVL 4729	Y
Maubeugia lotharingica	IRSNB R172	Y
Menadon besairiei	UA 10601 (Malagasy specimen); UFRGS-PV 0891T, 1164T (Brazilian specimens)	Y
Microscalenodon nanus	IRSNB R406	Y
Nanogomphodon wildi	SMNS 51962	Y
Pascualgnathus polanskii	PVL 4416	Y
Protuberum cabralense	MGB 368/100	Y
Rosieria delsatei	IRSNB R173	Y
Santacruzodon hopsoni	MCN PV 2752	Y
Scalenodon angustifrons	CAMZM T910	Y
Scalenodontoides macrodontes	MNHN 1957-23; BP/1/5395	Y
Sinognathus gracilis	IVPP V2339	N
Siriusgnathus niemeyerorum	CAPPA/UFSM 0032; CAPPA/UFSM 0125	Y
Titanogomphodon crassus	GSN R322	Y
Traversodon stahleckeri	GPIT/RE/1069, 7170; UFRGS-PV 0224T	Y
Traversodontidae indet.	CGP JSM 100, IRSNB R204	Y
Trirachodon berryi	BSP 1934 VIII 21; NHMUK R3307; SAM PK K171, K4801	Y

2.2 | Three-Dimensional modeling of the Gomphodont Postcanines

3D-models were generated for lower and/or upper postcanines in all examined taxa through photogrammetric techniques using Agisoft Photoscan Standard (Version 1.3.4; Software; 2017; retrieved from http://www.agisoft.com/downloads/installer/) and using photos taken with the portable microscope and digital camera (Figure 1b,c). The batch process followed in Agisoft Photoscan to reconstruct the postcanines in 3D consisted of four steps: (i) photos taken in all views were aligned using the standard options (i.e., with generic pre-selection and 40,000 key point limit and 4000 tie point limit) and with a medium-to-high accuracy for photos taken with the camera and the highest accuracy for photos taken with the

19328494, 2024, 4, Downloaded from https://anatomypubs.onlinelibrary.wiley.com/doi/10.1002/ar.25386 by University Of Witwatersrand, Wiley Online Library on [07/11/2024]. See the Terms and Conditions (https://onlinelibrary.wiley.com/terms-and-conditions) on Wiley Online Library for rules of use; OA articles are governed by the applicable Creative Commons License

digital microscope; (ii) a dense cloud was built in high to ultra-high quality with an aggressive depth filtering and no reuse depth map; (iii) the mesh was then built with a high face count and default options (i.e., a custom face count of 200,000 faces, arbitrary surface type, interpolation enabled and vertex color calculated); (iv) the texture was finally added using the default options (i.e., generic mapping mode, texture from all cameras, mosaic blending mode, texture size of 4096 and count of 1, no color correction and the hole filling option).

A total of 110 3D-models of gomphodont postcanines (i.e., 65 uppers and 45 lowers) belonging to 34 gomphodont taxa were created. 3D-models could not be generated for *Sinognathus* due to the occlusion and bad preservation of the postcanines, and for *Arctotraversodon*, *Beishanodon*, *Santagnathus*, *Scalenodon ribeiroae*, *Plinthogomphodon*, and *Ruberodon*, which could not be examined first hand. Although the holotype of *Guttigomphus avilionis* was examined by us, a 3D-model of the postcanine was not generated as the specimen was only recently considered as representing a new gomphodont taxon by Rayner et al. (2022). Conversely, we created 3D-models of the upper and lower postcanines of the juvenile trirachodontid specimen CGS JSM 100 (Hopson, 2005), interpreted as a new taxon of basal traversodontid by Hendrickx et al. (2020). Likewise, a 3D model of IRSNB R204, an isolated lower postcanine of an indeterminate traversodontid (Godefroit, 1999), was created and considered as a new taxon in this study. Because 3D-models of poorly preserved or strongly worn-out postcanines were excluded from this study, values of dental complexity obtained for the upper postcanines of *Etjoia*, *Massetognathus ochagaviae*, and *Scalenodontoides*, the lower postcanines of *Traversodon*, as well as both upper and lower postcanines of *Gomphodontosuchus* were not considered. The upper and/or lower postcanine complexity was measured for 32 of 37 gomphodont taxa with a well-preserved postcanine dentition (i.e., all gomphodonts other than *Arctotraversodon*, *Beishanodon*, *Impidens*, *Gomphodontosuchus*, *Massetognathus ochagaviae*, and *Sinognathus*; n.b., the gomphodont with a well-preserved dentition that could not be included being *Guttigomphus*, *Santagnathus*, *Scalenodon ribeiroae*, *Plinthogomphodon*, and *Ruberodon*), which accounts for 86.5% of all known gomphodont taxa published to date. All 3D-models are available in the Supporting Information S1 and can be provided upon request to the corresponding author.

2.3 | Dental complexity analysis

Postcanine complexity was quantified using geographic information system (GIS) analyses and orientation patch count (OPC; Evans et al., 2007; Wilson et al., 2012) on 3D crown surfaces of postcanines (Figure 1). A strict modus operandi was followed to evaluate postcanine complexity with consistency. A single postcanine, typically the best preserved from the dentition, was digitally isolated from the jaw using the free-form selection tool in Agisoft Photoscan and, for the 3D-models generated with a CT-scan, using the select faces tool in MeshLab v.1.3.4.5027 BETA (Cignoni et al., 2008; Cignoni & Ranzuglia, 2014; Figure 1b,c). The 3D-model was then converted into a nonbinary Stanford PLY file (.ply) and imported into MeshLab. All major fractures and taphonomic recesses and cavities present on the crown, especially in the models generated through CT-scan data, were digitally removed. 3D-models were then reconstructed in MeshLab v.1.3.4.5027 BETA with the Poisson Surface Reconstruction using an octree depth of 11, a solver divide of 10, and a sample per node and a surface offsetting of one (Figure 1d). The Poisson Surface Reconstruction not only enables to reconstruct accurately the missing surface and overall shape of the crown but also smooth the surface of the model. Smoothing the crown surface additionally helps eliminating the problem of post-mortem irregularities and surface coarseness that strongly affects dental complexity. Following Winchester's (2016) methodology, only the surface above the lowest point of the occlusal basin was considered. We also used the Visual Computer Graphic reconstruction tool in Meshlab to reconstruct the basalmost parts of the postcanines, in case the model could not be properly reconstructed using the Poisson tool. In case the polygons of the reconstructed portions were particularly large, we subdivided the mesh using the Butterfly Subdivision tool of Meshlab with the default options (three iterations, edge threshold). All models were oriented in a way that the occlusal surface is facing apically, with the labial, lingual and/or central cusps oriented perpendicular to the horizontal plane passing through the crown.

The R package MolaR 4.5 (Pampush et al., 2016) was used to perform the analysis of complexity on the resulting 3D-models. Dental complexity was measured by using the OPC (Evans et al., 2007). The software first determines the surface orientation at each pixel on the 3D-model, then group them into patches of contiguous pixels that are facing the same cardinal direction, to finally provide an OPC value by counting the number of patches in eight direction bins (Wilson et al., 2012; Figure 1). The OPC calculation was repeated eight times at rotations of multiples of 5.625° to reduce the effect of a specific tooth orientation. The mean of these repetitions, known as the OPC ratio (OPCR), was the variable used to determine dental complexity (Evans et al., 2007; Wilson et al., 2012; Winchester, 2016). OPCR was visualized using 10 increments of dental complexity of different

19328494, 2024, 4, Downloaded from https://anatomypubs.onlinelibrary.wiley.com/doi/10.1002/ar.25386 by University Of Witwatersrand, Wiley Online Library on [07/11/2024]. See the Terms and Conditions (https://onlinelibrary.wiley.com/terms-and-conditions) on Wiley Online Library for rules of use; OA articles are governed by the applicable Creative Commons License

colors, from blue for the simplest postcanines with the lowest OPCR values to purple for the most complex crowns with the highest OPCR values (Figure 2).

All models were decimated to 5000, 4000, 3000, 2000, and 1000 faces using MolaR, and dental complexity was measured for each model with a minimum of 5 and 10 faces. Models with 2000, 3000, and 4000 faces with a minimum of 10 faces were revealed to best reflect dental complexity in our sample. A mesh with less than 2000 faces significantly decreases the range of OPCR values and erased some dental features present on the crown surface such as cingular cuspules. Conversely, models with more than 4000 faces, or considering five faces on the mesh, led to anomalously high values of dental complexity in relatively simple models showing coarse or irregular crown surface (Supporting Information S1). Because some postcanines were particularly small (<5 mm) and 3D-models of less than 2500 faces were built for some specimens, values of dental complexity for models of 2000 faces with a minimum of 10 faces were considered in this study (Figure 1e,f). Analysis of dental complexity, however, provided the same range of values for models decimated to 2000, 3000, and 4000 faces with a minimum of 10 faces considered, with dental complexity only varying by a factor of 1 out of 10 increments of complexity (Supporting Information S1). Seven models belonging to four taxa (*Cricodon*, *Exaeretodon*, *Trirachodon*, and the indeterminate traversodontid IRSNB R204) gave three continuous increments of dental complexity, and the middle one was, therefore, chosen. Likewise, models of the same tooth created in medium and high resolution with Agisoft Photoscan, or using photogrammetry or CT-scan data, also provided relatively similar OPCR values when decimated to 2000 and 3000 faces (Supporting Information S1). Both R packages MolaR and Geomorph (Adams & Otárola-Castillo, 2013) were used to visualize the OPC on each postcanine model (Figure 1).

The postcanine complexity was visualized for each taxon on the phylogenetic trees in the form of a large square divided into four small squares, each colored with one of the 10 colors representing the increments of dental complexity (Figure 2). Upper and lower squares represent the complexity of the upper and lower postcanine teeth, whereas the left and right squares show the lowest and highest values of dental complexity, respectively. The ancestral state of dental complexity in four traversodontid subclades (i.e., Traversodontinae, Massetognathinae, Arctotraversodontinae, and Gomphodontosuchinae) was portrayed with the same square system and using the lowest and highest values of postcanine complexity measured in members of these clades (Figure 2).

Curves of general postcanine complexity and of upper and lower postcanine complexity through time were generated by plotting the mean OPCR values of all postcanines together, and all upper and lower postcanines taken separately for five time-bins of the Triassic (i.e., late Olenekian–early Anisian, late Anisian–early Ladinian, late Ladinian–early Carnian, late Carnian–early Norian, and late Norian–Rhaetian) based on the stratigraphic distribution of gomphodont taxa taken from the latest literature (see Supporting Information S1) as well as the most recent stratigraphic chart published online (ICS version 2023/06; Cohen et al., 2023). These time bins were chosen over the six main stages of the Triassic to increase the number of taxa per time bin and because the stratigraphic distribution of most gomphodonts covered halves of two stages. With nine taxa, the late Anisian–early Ladinian time bin has the highest number of taxa. Conversely, with four taxa each, the late Olenekian–early Anisian and late Carnian–early Norian are the time bins with the lowest number of taxa. Curves of dental complexity were compared to those of taxon richness calculated using both taxonomic and phylogenetic approaches (Lane et al., 2005) and body mass. Taxonomic diversity estimates were determined by counting the number of taxa observed at the specified time. Conversely, phylogenetic diversity estimates (PDEs), which are based on the relationships among taxa generated by cladistic analyses and calibrated by plotting trees on a stratigraphic scale, were measured by counting the number of taxa at each point of time using both observed stratigraphic ranges and inferred ranges like ghost lineages and range extensions (Barrett & Upchurch, 2005; Lane et al., 2005). Data on skull length was taken from the literature, and cranial length of taxa known from limited dental and cranial material was estimated using the postcanine width and regression equations (Supporting Information S1). The width of the upper and lower postcanines was indeed revealed to be well-correlated with cranial length for gomphodonts in which both variables were measured from the same individual.

3 | RESULTS

Values of postcanine complexity plotted on three phylogenetic trees representing alternative hypotheses of gomphodont relationships show the absence of a clear phylogenetic trend in both upper and lower postcanine complexities, especially in traversodontids (Figures 2–4). However, a decrease in both upper and lower postcanine complexity is observed during the radiation of traversodontids whereas an increase in upper postcanine complexity occurs with the emergence of gomphodontosuchines. In basalmost gomphodonts, higher values of postcanine complexity were measured in the basally branching

19328494, 2024, 4, Downloaded from https://anatomypubs.onlinelibrary.wiley.com/doi/10.1002/ar.25386 by University Of Witwatersrand, Wiley Online Library on [07/11/2024]. See the Terms and Conditions (https://onlinelibrary.wiley.com/terms-and-conditions) on Wiley Online Library for rules of use; OA articles are governed by the applicable Creative Commons License

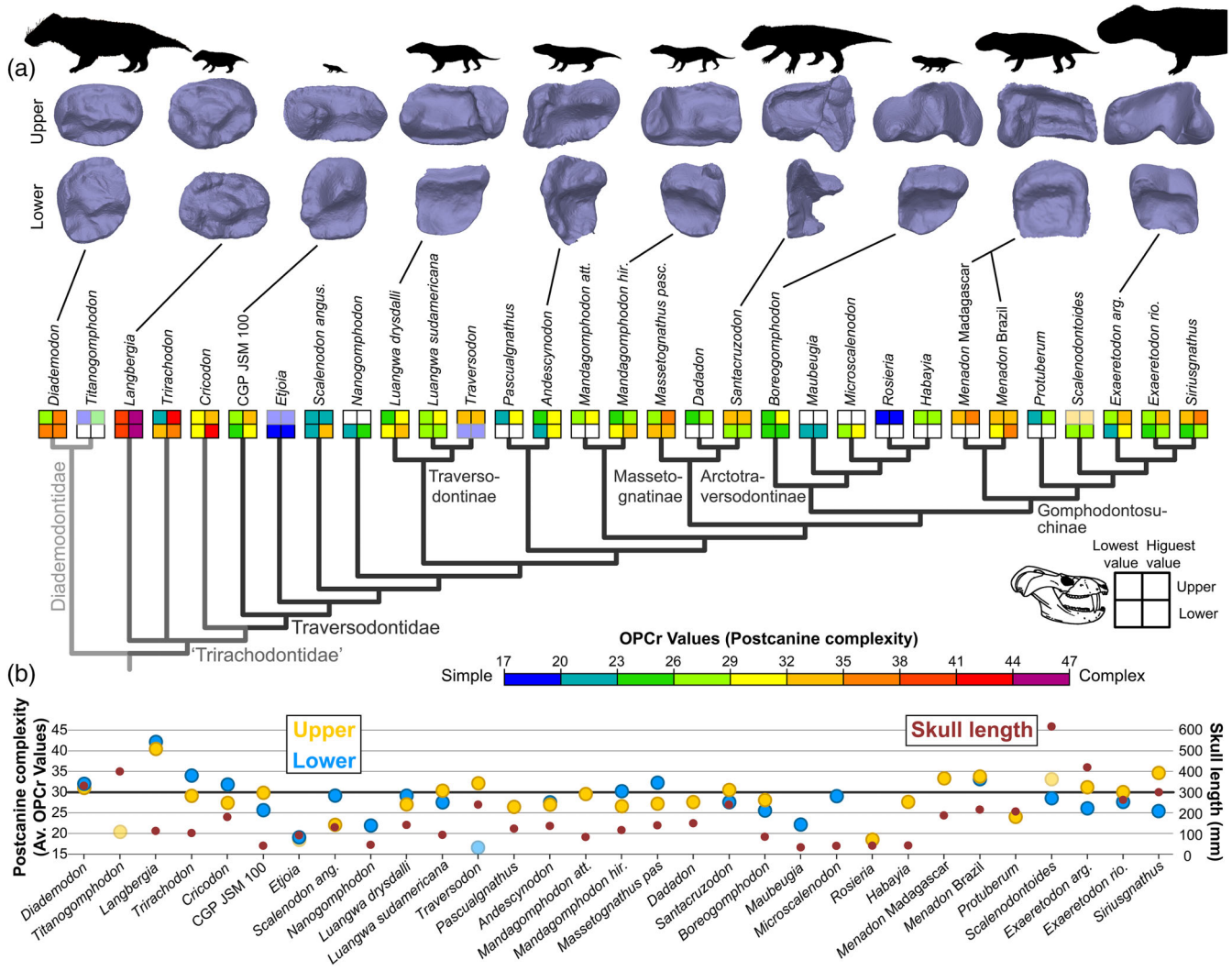


FIGURE 3 Postcanine complexity in gomphodont cynodonts. (a) Dental complexity visualized on the phylogenetic tree obtained by Schmitt et al. (2024) using Hendrickx et al. (2020) data matrix, based on 10 increments of complexity ranging from 17 to 47, the OPCR values obtained from 3D-models of postcanines decimated to 2000 faces with a minimum of 10 faces considered. The two upper and lower squares of each square represent the complexity of the upper and lower postcanines, respectively, whereas the left and right squares provide the lowest and highest values of dental complexity, respectively. Blurred/shaded squares (e.g. *Titanogomphodon*, *Etjoia*) illustrate dental complexity in particularly incomplete or worn-out postcanines. Black silhouettes of gomphodont taxa scaled using maximum skull length; (b) average dental complexity (quantified by the OPCR values) in upper (large orange dots) and lower (large blue dots) postcanines compared to the skull length (small purple dots) in gomphodont taxa. Black silhouettes credit: Gabriel Ugueto (CGP JSM 100) and José Eduardo Camargo Martínez (all others). Skull of *Pascualgnathus* on the left of the square modified from Martinelli (2010).

gomphodonts *Langbergia*, *Trirachodon*, and *Cricodon* (Figures 2 and 3a), classified among trirachodontids in some phylogenetic analyses (e.g., Rayner et al., 2022; Figure 4), whereas basalmost traversodontids have significantly lower dental complexity. Postcanine complexity remains high in basal gomphodonts placed nearby 'trirachodontids' such as *Diademodon* and the basalmost traversodontid CGP JSM 100 (Figures 2 and 3a). The highest values of dental complexity were obtained in *Langbergia*, the only gomphodonts whose OPCR values exceed 45 in upper and lower postcanines, and 40 in the average dental complexity for both upper and lower postcanines (Figure 3b). *Langbergia* is recovered as the basalmost gomphodont in Gaetano et al.'s (2022) phylogenetic tree (Figure 4), and a decrease in postcanine complexity is, therefore, seen in basalmost gomphodont following this topology. The lowest values of postcanine complexity (OPCR < 20) were measured in the lower postcanine of the basally branching traversodontid *Etjoia* and in the upper postcanine of the arctotraversodontine *Rosieria* (Figure 3b). Particularly low dental complexity is also recorded in the upper postcanine of *Scalenodon angustifrons* and the lower postcanine of the arctotraversodontine *Maubeugia*. Most other traversodontids display intermediate postcanine

19328494, 2024, 4, Downloaded from https://anatomypubs.onlinelibrary.wiley.com/doi/10.1002/ar.25386 by University Of Witwatersrand, Wiley Online Library on [07/11/2024]. See the Terms and Conditions (https://onlinelibrary.wiley.com/terms-and-conditions) on Wiley Online Library for rules of use; OA articles are governed by the applicable Creative Commons License

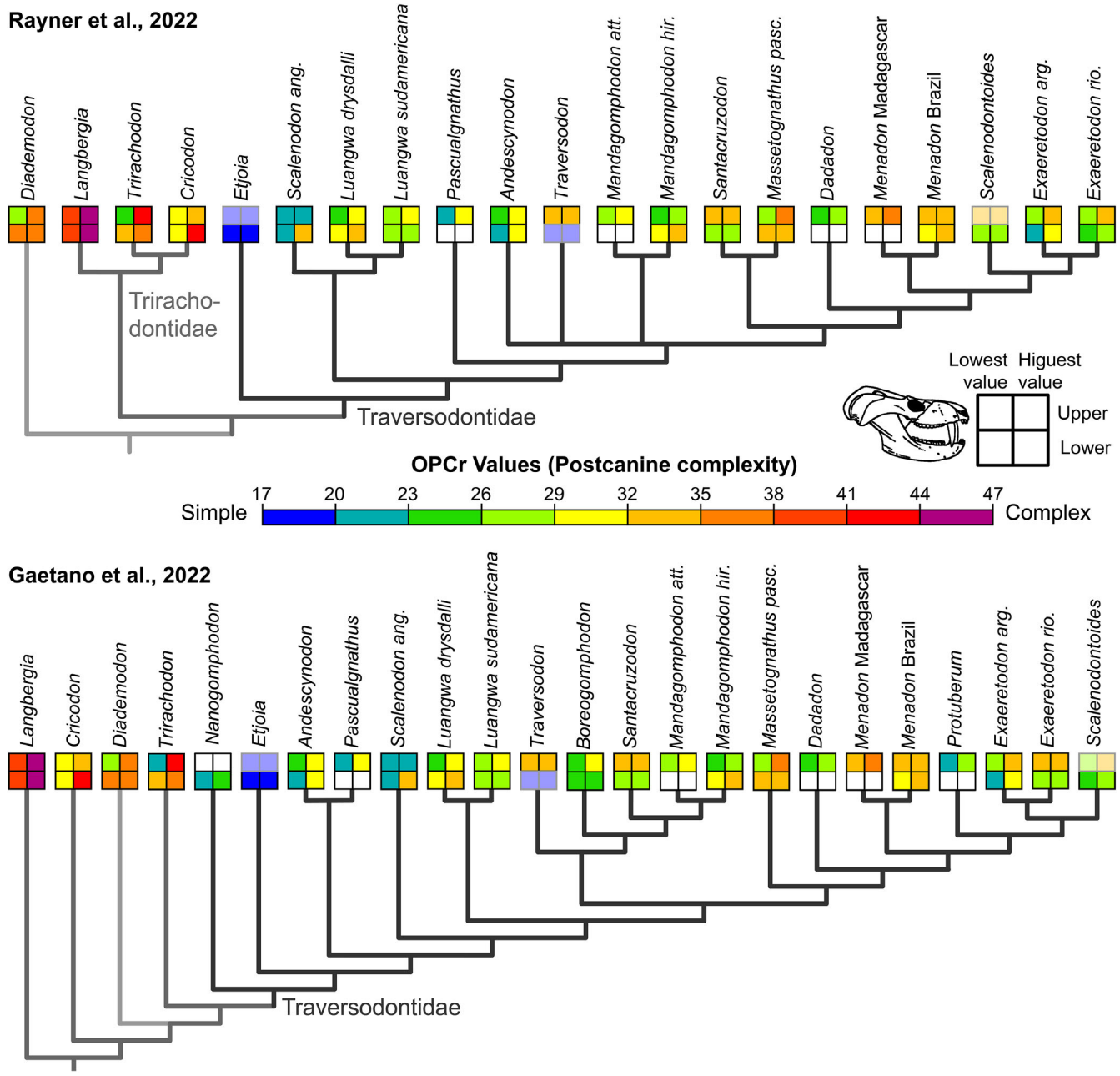


FIGURE 4 Postcanine complexity in gomphodont cynodonts visualized on the phylogenetic trees modified from Rayner et al. (2022; top) and Gaetano et al. (2022; bottom) based on 10 increments of complexity. Blurred/shaded squares (e.g., *Etjoia*, *Traversodon*) illustrate dental complexity in particularly incomplete or worn-out postcanines. Skull of *Pascualgnathus* on the left of the square modified from Martinelli (2010).

complexities, with OPCR values ranging from 23 to 35. Above-average values of upper postcanine complexity are found in some massetognathines such as *Massetognathus*, *Santacruzodon*, and in the gomphodontosuchines *Menadon* and *Siriusgnathus* (Figures 3b and 4). At the subclade level, arctotraversodontine traversodontids show lower dental complexity than traversodontines, massetognathines, and gomphodontosuchines (Figure 2).

A comparison of the mean OPCR values of upper and lower teeth (Figure 3b) indicates that postcanines from the upper and lower dentitions of a single species have relatively similar complexities to each other. The most important discrepancies between the upper and lower postcanine complexity are obtained in *Scalenodon angustifrons* and *Siriusgnathus*, whereas slight differences are measured in *Trirachodon*, *Cricodon*, and CGP JSM 100, as well as the traversodontids *Exaeretodon argentinus*, *Mandagomphodon*, *Massetognathus*, *Santacruzodon*, and *Boreogomphodon*. While dental complexity is higher in the upper postcanines of CGP JSM

19328494, 2024, 4, Downloaded from https://anatomypubs.onlinelibrary.wiley.com/doi/10.1002/ar.25386 by University Of Witwatersrand, Wiley Online Library on [07/11/2024]. See the Terms and Conditions (https://onlinelibrary.wiley.com/terms-and-conditions) on Wiley Online Library for rules of use; OA articles are governed by the applicable Creative Commons License

100, *Boreogomphodon*, and gomphodontosuchines, the reverse condition is present in trirachodontids, basalmost traversodontids more derived than CGP JSM 100, as well as *Mandagomphodon*, and *Massetognathus*. Interestingly, the two species of *Luangwa* show similar values of OPCR but opposite condition of dental complexity, with *L. drysdalli* and *L. sudamericana* having slightly more complex lower and upper postcanines, respectively (Figure 3b). Mapping the mean OPCR values also shows that nontraversodontid gomphodonts, *Massetognathus*, and *Mandagomphodon hirschsoni* have more complex lower postcanines, whereas CGP JSM 100, *Luangwa sudamericana*, *Santacruzodon*, *Boreogomphodon* and gomphodontosuchines have more complex upper postcanines. Comparing postcanine complexity with size, here quantified by the maximum skull length, does not show a clear correlation. High levels of dental complexity are found in small (i.e., skull length < 150 mm; *Langbergia*), medium (i.e., skull length of 150–300 mm; *Traversodon*, *Menadon*), and large-bodied gomphodonts (i.e., skull length > 300 mm; *Diademodon*, *Siriusgnathus*). Particularly small traversodontids (i.e., skull length < 100 mm) such as *Etjoia*, *Nanogomphodon*, *Maubeugia*, and *Rosieria* tend to have simple postcanines (not related with worn), although the basalmost and probably juvenile traversodontid CGP JSM 100 as well as the dwarves arctotraversodontines *Microscalenodon* and *Habayia* have more complex gomphodont teeth (Figure 3b).

Curves of postcanine complexity throughout the Triassic reveal that mean dental complexity in both upper and lower postcanines peaked in the late Olenekian–early Anisian. This was driven by the occurrence of high maximal complexity in taxa such as *Langbergia* and *Trirachodon*, and a scarcity of taxa with low complexity. This was followed by a significant drop of mean complexity in both the upper and lower dentitions during the late Anisian–early Ladinian (Figure 5a,b). General postcanine complexity then weakly increased in the late Ladinian–early Carnian and remained stable throughout the late Carnian–early Norian, before slightly diminishing during the late Norian–Rhaetian (Figure 5a). Minimum complexity occurred at the end of the Triassic, but mean OPCR values of postcanine complexity for this interval were only slightly lower than those in the late Anisian–early Ladinian (Figure 5a). Upper and lower postcanine complexities follow opposite trends in the Middle and Late Triassic, with an increase in complexity from the late Anisian–early Ladinian to the late Carnian–early Norian in the upper dentition, while lower postcanines diminish in complexity during the same period of time (Figure 5b). Postcanine complexity and disparity in postcanine complexity follow the same general trends throughout the Triassic. The highest amount of disparity in dental complexity is indeed found in the late Olenekian–early Anisian in both the upper and lower postcanines, whereas the lowest level of disparity is measured at the end of the Triassic (Figure 5a, b). Disparity in upper postcanine complexity, however, increases from the early Ladinian to the late Carnian (Figure 5b), an age in which general complexity values are constant (Figure 5a).

Peaks in dental complexity and disparity in postcanine complexity in the Early Triassic occur when gomphodonts had low species richness, as estimated both by counting taxa within an interval (taxonomic richness) or by counting species plus phylogenetic ghost lineages (the PDE), which happens much later in the early Carnian. Gomphodont tooth complexity additionally sharply decreases during the Anisian, when an increase in phylogenetic diversity and taxonomic richness is recorded (Figure 5a) and remains stable between the late Ladinian and early Norian while a decrease in phylogenetic diversity and taxonomic richness occurred from the late Carnian to the late Norian. Maximum body size in gomphodonts was recorded during the late Carnian–early Norian when postcanine complexity remained stable. Dental complexity diminishes in the late Anisian and slightly increases in the Ladinian, while the reverse occurs with body size, which slightly increases and decreases during the same period of time (Figure 5c). The same trends, however, are observed in the Late Triassic when postcanine complexity, phylogenetic diversity, taxonomic richness, and mean cranial length all decrease from the late Carnian to the Rhaetian.

4 | DISCUSSION

4.1 | Early rise of postcanine complexity and feeding ecologies in basal gomphodonts

Results of the analysis of dental complexity clearly reveal that the peak in gomphodont postcanine complexity was reached during the earliest evolutionary history of gomphodont cynodonts (Figure 2). Maximum postcanine complexity was indeed measured during the late Olenekian–early Anisian interval (Figure 5a,b) during which *Diademodon*, *Langbergia*, *Trirachodon*, and the basalmost traversodontid GSM JSM 100 inhabited the Southern Hemisphere. The most complex gomphodont teeth are in fact found in the oldest gomphodont taxa of our sample. *Langbergia* and *Trirachodon* come from the Olenekian and both show the most complex upper and/or lower postcanines (Figure 2). *Langbergia* and *Trirachodon* (also *Beishanodon* with poorly preserved

19328494, 2024, 4, Downloaded from https://anatomypubs.onlinelibrary.wiley.com/doi/10.1002/ar.25386 by University Of Witwatersrand, Wiley Online Library on [07/11/2024]. See the Terms and Conditions (https://onlinelibrary.wiley.com/terms-and-conditions) on Wiley Online Library for rules of use; OA articles are governed by the applicable Creative Commons License

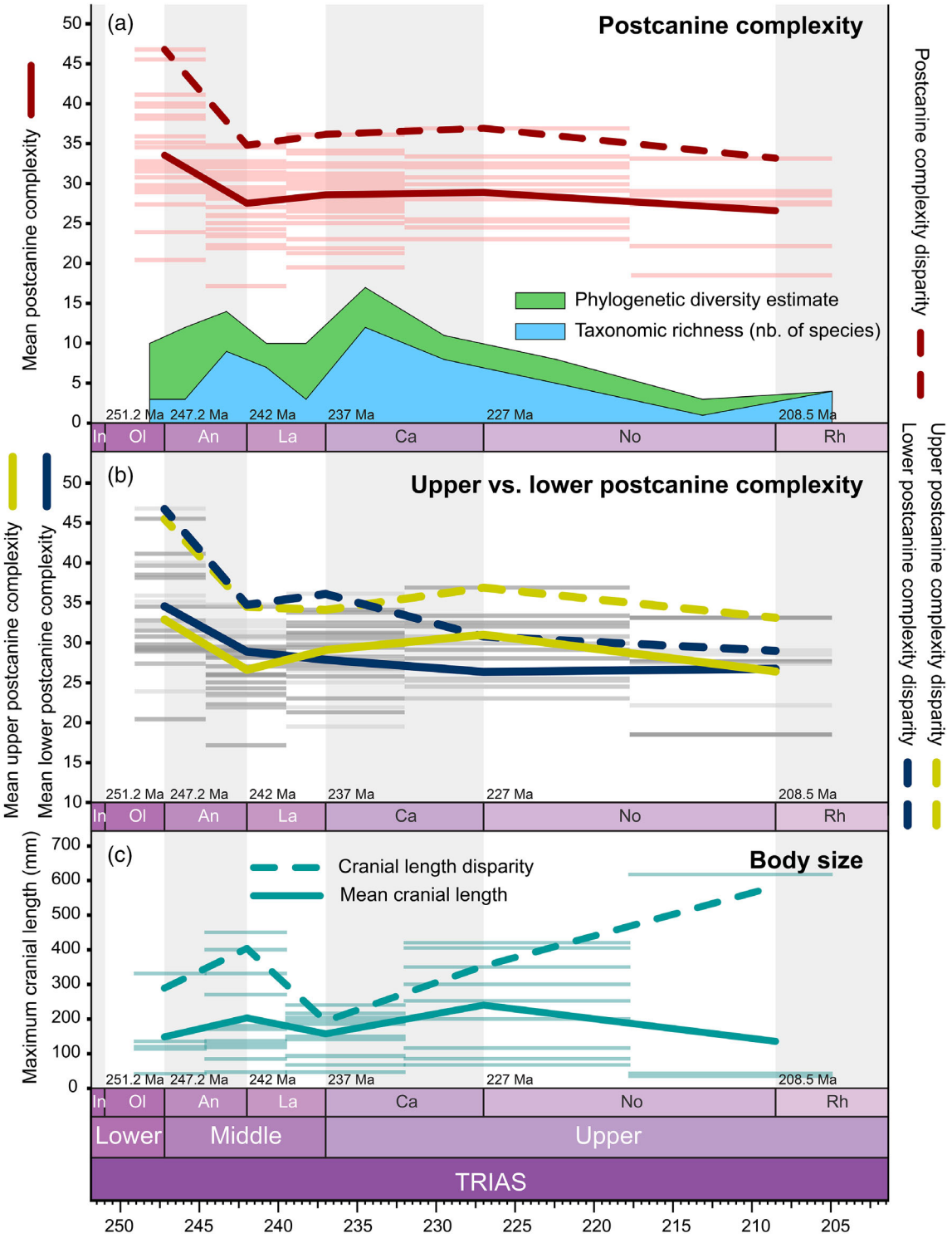


FIGURE 5 Evolution of postcanine complexity in gomphodont cynodonts throughout the Triassic. (a) Mean dental complexity (dark red continuous line) and disparity in dental complexity (dark red dashed line) in five stratigraphic bins of the Triassic, compared to the phylogenetic diversity (in green) and taxonomic richness (in blue) of gomphodont cynodonts. Light red horizontal bars in each five time-bin represent OPCR values of dental complexity from our sample; (b) mean upper (dark yellow continuous line) and lower (dark blue continuous line) postcanine complexity as well as disparity in the upper (dark yellow dashed line) and lower (dark blue dashed line) dental complexity in five stratigraphic bins of the Triassic. Light and dark gray horizontal bars represent OPCR values of upper and lower postcanine complexity from our sample, respectively; (c) mean cranial length (continuous line) and disparity in cranial length (dashed line) in five stratigraphic bins of the Triassic. Horizontal bars represent the cranial lengths of gomphodont taxa from each five time-bin.

19328494, 2024, 4, Downloaded from https://anatomypubs.onlinelibrary.wiley.com/doi/10.1002/ar.25386 by University Of Witwatersrand, Wiley Online Library on [07/11/2024]. See the Terms and Conditions (https://onlinelibrary.wiley.com/terms-and-conditions) on Wiley Online Library for rules of use; OA articles are governed by the applicable Creative Commons License

postcanines) are in some phylogenetic schemes included among the clade Trirachodontidae (e.g., Rayner et al., 2022; Figure 4), whose members are characterized by upper and lower postcanines with centrally positioned transverse ridge made of three well-separated cusps (i.e., the labial, central, and lingual cusps) and ringed by distinctive cingular cuspules (Hendrickx et al., 2019, 2020; Hopson & Kitching, 1972; Sidor & Hopson, 2018). The high dental complexity measured in this group is, therefore, the combined result of well-defined labial, central, and lingual cusps, with a cingulum bearing numerous (tiny or large) cuspules on the mesial and distal margins of the postcanines (Figures 1k and 3). *Langbergia*, the gomphodont with the most complex upper and lower postcanines, is diagnosed by subcircular postcanines with globulous cusps and cingular cuspules sharing the same size (Figure 3a), which explains the particularly high values of dental complexity recorded for this taxon. The unusual morphology of the trirachodontid postcanines, unseen in any extant animals, led authors to suggest a peculiar feeding ecology for these gomphodonts. Hopson and Kitching (1972) and Reisz and Sues (2000) interpreted them as omnivores or herbivores whereas Gow (1978) considered them as insectivores or carnivores based on the piercing and cutting functions of the postcanines. Based on the general dentition morphology of the group, Hendrickx et al. (2020) assumed that trirachodontids were likely adapted to a specialized feeding ecology involving small and particularly hard plant material and/or prey items such as ground-living insects with hard exoskeletons. High values of postcanine complexity in gomphodonts are, therefore, linked with nonstrictly herbivorous and probably omnivorous and partially insectivorous feeding ecology.

Unlike trirachodontids, basalmost traversodontids from the late Anisian–early Ladinian interval such as *Andescynodon*, *Mandagomphodon*, *Nanogomphodon*, and *Scalenodon angustifrons* are characterized by the loss of conspicuous cingular cuspules and the presence of wide mesial and/or distal occlusal basins occupying most of the upper and lower postcanines, resulting in lower values of dental complexity (Figure 5a,b). A tendency toward simplicity was also observed in the whole dentition of basal traversodontids by Hendrickx et al. (2020), who associated this trend to a gradual change in dietary niches, from a carnivorous/omnivorous to a more herbivorous feeding ecology, during the early radiation of Traversodontidae (see also Crompton, 1972; Reisz & Sues, 2000). Hendrickx et al. (2020) argued that basalmost traversodontids such as *Etjoia* and the putative traversodontid CGP JSM 100, which have an intermediate postcanine morphology between the trirachodontid puncturing type and the traversodontid shearing type, were probably omnivores, dealing with a larger amount of plant material than non-neogomphodont gomphodonts. The presence of transversely and longitudinally oriented shearing planes in the closely related *Scalenodon angustifrons* and *Mandagomphodon*, with jaw movements either upward and backward (*Scalenodon*) or forward and backward (*Mandagomphodon*) during mastication (Crompton, 1972; Hopson, 2014), however, suggests that these two basal traversodontids and other closely related taxa such as traversodontines, *Pascualgnathus*, and *Andescynodon*, were predominantly, if not strictly herbivorous (Brink, 1963; Crompton, 1972; Gow, 1978; Hendrickx et al., 2020; Hopson & Kitching, 1972; Kemp, 1980). Filippini et al. (2022) recently hypothesized the fact that small-bodied traversodontids (i.e., skull length of <150 mm) like *Pascualgnathus* and *Andescynodon* had skull and dental morphologies suggestive of highly nutritious food items and may have, therefore, been generalist cynodonts. An exclusively herbivorous feeding ecology, however, appears to have been present in the larger and more derived traversodontids Massetognathinae and Gomphodontosuchinae (e.g., Melo et al., 2019; Wynd et al., 2022), which were hypothesized to have had a generalized and specialized herbivorous diet, respectively, by Filippini et al. (2022).

Interestingly, the connection between insectivory/omnivory with high postcanine complexity and herbivory with lower dental complexity contrast with the trends of complexity observed in the dentition of living saurians (Christensen & Melstrom, 2021; Melstrom, 2017), Mesozoic crocodyliforms (Melstrom & Irmis, 2019), dinosaurs (Melstrom et al., 2021), and, among mammals, bats (Santana et al., 2011), carnivorans and rodents (Evans et al., 2007). In reptilians such as lizards, crocodyliforms, and dinosaurs, the teeth of herbivorous forms, which are either labiolingually expanded with ridges, and minute cuspules or folidont (leaf-shaped) and with a row of well-defined cusps, are more complex that those of carnivorous forms with simple ziphodont (i.e., blade-shape) or conidont (i.e., conical) teeth (Hendrickx et al., 2015; Melstrom, 2017; Melstrom et al., 2021). Among cynodonts, teeth with well-defined crests are recovered as simpler in gomphodonts, whereas in living mammals, such as rodents and carnivorans, bunodont cusped teeth are simpler than crested postcanines (Evans et al., 2007). However, the crests in the dental series of living mammals studied by Evans et al. (2007) show intricate patterns that fold and change of direction, whereas the coalescence of large cusps in traversodontids typically produce one transverse and one labial crests, both disposed lineally. Considering the fact that dental complexity is a measure of breaking sites for the food on the crown (Evans et al., 2007), the presence of numerous separated cusps and cuspules is indeed an amplification of the complexity due to the increase of possible breakage sites. High values of postcanine complexity in

19328494, 2024, 4, Downloaded from https://anatomypubs.onlinelibrary.wiley.com/doi/10.1002/ar.25386 by University Of Witwatersrand, Wiley Online Library on [07/11/2024]. See the Terms and Conditions (https://onlinelibrary.wiley.com/terms-and-conditions) on Wiley Online Library for rules of use; OA articles are governed by the applicable Creative Commons License

gomphodonts is indeed reflecting the presence of independent cusps of different sizes widely distributed along the crowns that do not coalesce to form crests or superstructures, the dental condition observed in the "trirachodontid" postcanines. OPCR values are not so high for *Diademodon*, which also have relatively independent cusps but not as conspicuous as in trirachodontids. Besides cusp coalescences forming crests, the development of deep basins in the postcanines implies more uniform reflections of the OPCRs simplifying the perceived pattern of the crown. The complexity in near all traversodontids show average values close to 30 OPCR (Figures 2 and 3b), with a major divergence in the simplicity of the upper postcanines of *Rosieria* and the lower postcanines of *Nanogomphodon*, *Maubeugia*, and *Etjoia*, the first three being dwarf traversodontids from Europe (Godefroit, 1999; Godefroit & Battail, 1997).

In Middle Triassic biomes humidity became slightly higher than in the Early Triassic and seasonal semiarid conditions in South Pangea (Donnadieu et al., 2006; Mancuso et al., 2021), allowed re-establishing multistorey vegetation ensuring a heterogeneous ecosystem. Most extensive plant communities were formed, and the *Dicroidium* flora began to establish as the dominant components, although some elements of Northern Pangean floras were mixed in South Pangea (Cariglino et al., 2016, 2018). This environment and flora accompanied the first taxonomic diversification of Cynognathians, with the development of different patterns of gomphodont postcanines along with a diversification of diets, and the acquisition of larger body sizes.

4.2 | Herbivory and stasis of traversodontid dental complexity

The increase in plant material and gradual trend toward a strictly herbivorous diet in Traversodontidae was not accompanied by a conspicuous change in general postcanine complexity in the Middle and Late Triassic (Figure 5a). Dental complexity and disparity in dental complexity are low in periods of high diversity in gomphodonts (Figure 5a). The first peak of diversity in this group occurred in the late Anisian and is correlated with low values of postcanine complexity and disparity in postcanine complexity, whereas the second peak of diversity in the Early Carnian is followed by a subtle increase in disparity and general postcanine complexity. This is reflected in the development of the traversodontids postcanines, made of crests and basins, which are clearly less complex than those of more basal gomphodonts. Once the traversodontid pattern is established, there are few changes in complexity from the late Anisian to the Carnian.

An increase in complexity in the upper postcanine is, nevertheless, observed in the late Carnian–early Norian (Figure 5b), a peak explained by the relatively high values of upper postcanine complexity obtained in *Exaeretodon* and *Siriusgnathus* (~32, with 36.9 in one of *Siriusgnathus*' upper postcanines) and a lower number of traversodontids with simpler upper postcanines. High postcanine complexity in these two gomphodontosuchines results from the combined presence of an extensively developed shouldering, protuberant labial and lingual cusps, and a well-separated labiodistal accessory cusp (Figure 1o), a combination of dental features observed in the distalmost upper gomphodont postcanines of derived gomphodontosuchines (Goñi & Goin, 1991). Shouldering, the mesial projection of the mesiolabial border of the upper postcanine resulting in a 'shoulder'-like process on the preceding tooth (Figure 1m,o), is a major dental feature differentiating basal from derived traversodontids (Abdala & Ribeiro, 2003; Romer, 1967) and contributing in the dental complexity of derived traversodontids. Absent in basal traversodontids like traversodontines, *Pascualgnathus*, *Andescynodon*, *Mandagomphodon*, and *Scalenodon ribeiroae*, a shouldering is incipiently developed in massetognathines, some arctotraversodontines (*Boreogomphodon*, *Plinthogomphodon*, *Habayia*), and basal gomphodontosuchines (*Menadon*, *Gomphodontosuchus*), whereas an extensive shouldering characterizes the upper postcanines of derived gomphodontosuchines such as *Scalenodontoides*, *Exaeretodon*, *Siriusgnathus*, and *Santagnathus* (n.b., the basal gomphodontosuchine *Protuberum* and the arctotraversodontines *Rosieria* and *Microscalenodon* are devoid of a shouldering; Abdala & Ribeiro, 2003; Abdala et al., 2006; Abdala & Sa-Teixeira, 2004; Hopson, 1985; Liu & Sues, 2010; Martinelli, 2010; Melo et al., 2015, 2017; Miron et al., 2020; Pavanatto et al., 2018; Ranivoharimanana et al., 2011; Reichel et al., 2009; Schmitt et al., 2024). Functionally, the presence of a shouldering resulted in the development of a more extended occlusal basin and obliquely orientated crests enabling a wider tooth surface for food gridding. Larger crushing and grinding surfaces indicate that traversodontids with this dental feature had a greater capacity to process food per masticatory cycle. The dentition of Gomphodontosuchinae suggests that they were capable of processing a large amount of plant material. Derived gomphodontosuchines such as *Exaeretodon*, *Siriusgnathus*, and *Scalenodontoides* are the largest traversodontids known to date, reaching body weights greater than 100 kg (Filippini et al., 2022). Extant herbivorous mammals of similar size are known to consume large amounts of structural plant material such as leaves and stems (Pineda-Munoz et al., 2016), a similar type of diet that might have been shared by these

19328494, 2024, 4, Downloaded from https://anatomypubs.onlinelibrary.wiley.com/doi/10.1002/ar.25386 by University Of Witwatersrand, Wiley Online Library on [07/11/2024]. See the Terms and Conditions (https://onlinelibrary.wiley.com/terms-and-conditions) on Wiley Online Library for rules of use; OA articles are governed by the applicable Creative Commons License

large-bodied gomphodontosuchines. Representatives of this group show conspicuous cranial and functional adaptations to chewing hard plant material such a strictly palinal (i.e., backward) movement of the lower jaw (Kubo et al., 2017) as well as robust and high horizontal rami, a huge, tall coronoid process with the dorsal margin located above the zygomatic arch, deep zygomatic arches (more massive than in the majority of other traversodontids), and enlarged temporal fenestrae (Bonaparte, 1962; Liparini et al., 2013; Wynd et al., 2022). These features are indicative of the development of a powerful occlusal musculature (Crompton & Attridge, 1986; Reisz & Sues, 2000).

Conversely, the diminution in lower postcanine complexity occurring from the late Olenekian–early Ladinian to the late Carnian–early Norian (Figure 5b) can be explained by the gradual loss, throughout the evolutionary history of Traversodontidae, of dental features directly participating in dental complexity in more basal gomphodonts: a mesial basin and a central cusp in the transverse crest in basal traversodontids, well-defined cingular cuspules in traversodontids more derived than massetognathines, and a mesial cingulum and well-separated accessory cuspules in gomphodontosuchines (Hendrickx et al., 2020). The minimum lower postcanine complexity achieved in the late Carnian–early Norian results from the particular simplicity in the lower postcanines of derived gomphodontosuchines like *Exaeretodon* and *Siriusgnathus*. The lower gomphodont postcanines of these taxa indeed only consist of subquadrangular crowns with a large distal basin occupying most of the crown and mesially bounded by a tall transverse crest made of the labial and lingual cusps (Figure 3a). Unlike the upper postcanines, there is no shouldering nor strongly protuberant cusps and well-separated cuspules in the lower postcanines of derived gomphodontosuchines, and such a difference in morphology explains the discrepancy in complexity between the upper and lower postcanines of these traversodontids (Figures 2 and 3b).

The slight decrease in both general and upper postcanine complexities during the Late Triassic is the result of the presence of dwarf arctotraversodontine with simple postcanines in Europe during the Rhaetian (Godefroit, 1999; Godefroit & Battail, 1997; Hahn et al., 1988; Figures 2 and 3). If the gomphodont postcanines of *Microscalenodon* and *Habayia* have average values of dental complexity among traversodontids, the upper and lower postcanines of *Rosieria* and *Maubeugia*, respectively, are particularly simple (Figure 3). The difference in dental complexity between these taxa is, however, difficult to explain. All four are characterized by particularly large and bulbous cusps as well as shallow and poorly delimited basins, which contrast with the gomphodont postcanines of other traversodontids such as the basally branching arctotraversodontine *Boreogomphodon*, with narrower transverse crest and smaller cusps. Simplicity in the postcanines of *Rosieria* and *Maubeugia* appears to be due to the particularly large size and importance of their cusps (the lingual one in *Rosieria*, and the labial, lingual and mesiolabial ones in *Maubeugia*), which occupy most of the crown surface (this condition, however, contrasts with that of *Langbergia* whose postcanines bear multiple bulbous cusps and cingular cuspules directly participating in the high values of dental complexity measured in this taxon). *Habayia*, *Maubeugia*, *Microscalenodon* and *Rosieria* all lived in Northwestern Europe, which was transformed into an archipelago of small islands by the Rhaetian transgression leading to insular dwarfism (Godefroit, 1999; Godefroit & Battail, 1997). Godefroit and Battail (1997) and Godefroit (1999) suggested that the peculiar gomphodont dentition of these traversodontids was for a specialized diet of hard plant material in an environment where vegetation was dense and gomphodonts occupied a particular niche to avoid competition with other more abundant herbivorous cynodonts (i.e., Haramyidae and Theroteinidae). Dwarf traversodontids were, however, a rare component of this island ecosystem and a direct competition with herbivorous mammals having a more advanced physiology (Araújo et al., 2022; Godefroit & Battail, 1997), combined with an over-specialized dietary niche, probably led to their extinction at the end of the Triassic.

The traversodontid dentition is made of rows of labiolingually expanded postcanines with transversally oriented crests and working as a unit during propalinal movement of the jaws when chewing (Crompton, 1972; Goswami et al., 2005; Gow, 1978; Hopson, 2014; Kubo et al., 2017). A group of extant mammals presenting a somewhat similar dental morphology is caviomorph rodents such as chinchillas, nutrias, capybaras, and New World porcupines. These mammals present multiple crests perpendicular to the dental row, but with the same tooth presenting several crests or lophs, with a total of four functional teeth per row (i.e., one premolar and three molars). This type of dental feature, along with the presence of a homogeneous morphology of the cheek teeth, is associated with grinding function and herbivory (Boivin et al., 2022). Conversely, traversodontids bear a single crest per postcanine and also have numerous gomphodont postcanines with the same structure (Massetognathinae: 6–18; Gomphodontosuchinae: 5–10; Hendrickx et al., 2020; Liu & Abdala, 2014). Although caviomorphs are adapted to more extended propalinal movements, these rodents and traversodontids both present jaw movements with predominant palinal directions, which allow the tooth row to shear, crush, and grind food, suitable for processing a large amount of plant material per masticatory cycle. Conversely

19328494, 2024, 4, Downloaded from https://anatomypubs.onlinelibrary.wiley.com/doi/10.1002/ar.25386 by University Of Witwatersrand, Wiley Online Library on [07/11/2024]. See the Terms and Conditions (https://onlinelibrary.wiley.com/terms-and-conditions) on Wiley Online Library for rules of use; OA articles are governed by the applicable Creative Commons License

to caviomorph rodents, which have fewer teeth and more complex crowns, gomphodonts became functionally specialized to an herbivory diet by reducing dental complexity and maintaining a large number of postcanine teeth per tooth row. It should, however, be noted that among different caviomorph lineages, there are trends in reducing the number of lophs (Boivin & Marivaux, 2020 and references therein), and the reduction of crests in tooth crown is not entirely unseeing in mammalian lineages. Therefore, dental complexity alone is not strictly associated with diet specialization.

In the first half of the Late Triassic, Southern Pangea was dominated by seasonal subhumid conditions with one or more semi-arid intervals and an increase in precipitation by the 'Carnian Pluvial Episode' (Benavente et al., 2021; Mancuso et al., 2020, 2021). This regime allowed for the climax of *Dicroidium* flora (Bomfleur et al., 2018) with the domination of conifers, with other types of gymnosperms, ferns, and sphenophytes as subordinate elements of the vegetation assemblage (Kustatscher et al., 2018; Spalletti et al., 2003). At this time, traversodontids present a relatively stable postcanine complexity with a traversodontid type of pattern (i.e., gomphodont postcanines with wide basins, mesially or distally displaced transverse crests, and cingula either absent or made with poorly delimited cingular cuspules) established, along with the development of a shouldering. These features enabled them to attain a specialized herbivorous diet and to reach larger body sizes.

5 | CONCLUSIONS

These are the first analyses on morphological complexity in the postcanines of gomphodont cynodonts, the dominant group of cynodonts in southern Pangaea during the Middle and Late Triassic, using quantitative data. The study used GIS analysis and OPC on 3D models of crown surfaces of both upper and lower gomphodont postcanines in 32 gomphodont taxa. Our analyses are limited to gomphodont (i.e., labiolingually expanded) postcanines, which are the dominant dental elements in the majority of gomphodont taxa. We found that the peak in postcanine complexity was reached early in the evolution of Gomphodontia, with the irruption of omnivorous or insectivorous forms ("trirachodontids") with heavily cuspidate postcanines in the Early Triassic. The successful radiation of Middle Triassic traversodontids, however, led to a sharp decrease in postcanine complexity due to the coalescence of cusps into transversal and labial crests and the development of large occlusal basins. This simplification in the gomphodont postcanines is interpreted as related to a gradual increase in the consumption of plant material. The connection between insectivory/omnivory with high postcanine complexity and herbivory with lower dental complexity in gomphodonts is, therefore, in opposite way to the trend of dental complexity observed in living saurians, Mesozoic crocodyliforms, dinosaurs, and some extant mammals such as bats and rodents. Postcanine complexity remained relatively stable throughout the evolution of traversodontids but slightly diminished in the Late Triassic due to the presence of dwarf forms with particularly simple gomphodont postcanines in the Rhaetian.

There is an apparent association between the acquisition of feeding specialization and taxonomic diversification in gomphodonts with the *Dicroidium* flora assemblage dominance. This link provides further explanation for the Southern Pangean distribution of gomphodonts, as the Late Triassic floras of the southern landmasses are homogenous compared with the Northern Hemisphere vegetation, which presented several floristic subprovinces. Simplification of postcanines along with homogenization of the dental row allowed gomphodonts to explore new ecological niches and acquire a wider range of body sizes. Likewise, dental specialization to herbivory and feeding on this distinctive floral assemblage resulted in gomphodonts being unable to adapt when floristic composition changed toward the end of the Triassic.

This study on dental complexity using 3D models and OPC is the first to be done in nonmammaliaform synapsids. It opens the door to new investigations into the postcanine complexity in nonmammalian therapsids and its possible correlation with feeding strategies, body size, metabolism, phylogenetic diversity, floral changes, and major extinction events. Comparison between the postcanine complexity, dental disparity, and rates of dental evolution would also be a crucial addition to our knowledge on the evolution of the dentition of Gomphodontia and other nonmammalian synapsids.

AUTHOR CONTRIBUTIONS

Christophe Hendrickx: Conceptualization; investigation; funding acquisition; writing – original draft; methodology; validation; visualization; writing – review and editing; formal analysis; data curation. **Fernando Abdala:** Conceptualization; investigation; writing – original draft; supervision; writing – review and editing; methodology; funding acquisition; validation; project administration; resources. **Florencia S. Filippini:** Writing – original draft; investigation; writing – review and editing. **Simon Wills:** Methodology; software. **Roger Benson:** Writing – review and editing; data curation; resources. **Jonah N. Choiniere:** Supervision; conceptualization; resources; funding acquisition; software; project administration.

19328494, 2024, 4, Downloaded from https://anatomypubs.onlinelibrary.wiley.com/doi/10.1002/ar.25386 by University Of Witwatersrand, Wiley Online Library on [07/11/2024]. See the Terms and Conditions (https://onlinelibrary.wiley.com/terms-and-conditions) on Wiley Online Library for rules of use; OA articles are governed by the applicable Creative Commons License

ACKNOWLEDGMENTS

The postcanine dentition of a large number of gomphodont specimens was examined in several institutions of Argentina, Belgium, Brazil, China, England, France, Germany, Namibia, South Africa, and the USA, and access to material was possible thanks to the help and assistance of (by alphabetical order) Agustín Martinelli (MACN-Pv), Alejandro Kramarz (MACN-Pv), Alejo Scarano (MLP), Amanda Millhouse (USNM), Ana Maria Ribeiro (MCN), Annelise Folie (IRSNB), Bernard Zipfel (ESI), Carl Mehling (AMNH), Cesar Leandro Schultz (UFRGS), Daniel L. Brinkman (YPM), Elize Butler (NMQR), Feng Li (IVPP), Flávio Augusto Pretto (CAPPA/UFSM), Gertrud Rößner (BSP), Helke Mocke (GSN), Ingmar Werneburg (EKU), Jaime Powell (PVL), Jennifer Botha-Brink (NMQR), Jingmai O'Connor (IVPP), John J. Flynn (AMNH), Leonardo Kerber (CAPPA/UFSM), Lizhao Zhang (IVPP), Marcelo Reguero (MLP), Marco Brandalise de Andrade (PUCRGS), Marina Bento Soares (UFRGS), Mark Norell (AMNH), Martín Ezcurra (MACN-Pv), Mathew Lowe (CAMZM), Matthew Carrano (NMNH), Oliver Rauhut (BSP), Pablo Ortiz (PVL), Pascal Godefroit (IRSNB), Paul Barrett (NHM), Rainer Schoch (SMNS), Rodrigo González (PVL), Ronan Allain (MNHN), Sandra Chapman (NHM), Sifelani Jirah (ESI), Tomaz Melo (UFRGS), Xu Xing (IVPP), Zaituna Erasmus (SAM), and Zheng Fang (IVPP). We are also particularly thankful to Tomaz Melo for taking a large number of photos of *Protuberum* to reconstruct its dentition in 3D, technician Charlton Dube (ESI) for preparing the postcanine of a specimen of *Massetognathus*, Gabriel Ugueto for allowing us to use his reconstruction of *Massetognathus*, and Agustín Martinelli for pointing out the presence of PVL specimens in Porto Alegre. Last but not least, we thank Agustín Martinelli and an anonymous reviewer, as well as Assistant Editor Leonardo Kerber for their valuable corrections and suggestions which help improving this contribution. This research was financially supported by the DST-NRF Centre of Excellence, Palaeosciences, grants PPD2015/17CH and CoE2017-038, the Postdoctoral Fellowship from the University Research Committee (URC) of the University of the Witwatersrand, as well as the Consejo Nacional de Investigaciones Científicas y Técnicas (CONICET) and Agencia Nacional de Promoción Científica y Tecnológica, Argentina (Beca Pos-doctoral CONICET Legajo 181417), to Christophe Hendrickx; the Palaeontological Scientific Trust (PAST), the DST-NRF Centre of Excellence, Palaeosciences, an NRF African Origins Platform (AOP) grant (#98800), and an NRF Competitive Support for Rated Researchers (CPRR) grant to Jonah Choiniere (#98906); and the NRF, CONICET and Agencia Nacional de Promoción Científica y Tecnológica, Argentina (PICT 2020–01498) to Fernando Abdala. C.H. dedicates this work to Maria I. Martin.

ORCID

Christophe Hendrickx https://orcid.org/0000-0002-8500-2405

Simon Wills https://orcid.org/0000-0002-2012-1016

REFERENCES

Abdala, F. (2007). Redescription of *Platycraniellus elegans* (Therapsida, Cynodontia) from the Lower Triassic of South Africa, and the cladistic relationships of Eutheriodonts. *Palaeontology*, *50*, 591–618. https://doi.org/10.1111/j.1475-4983.2007.00646.x

Abdala, F., & Gaetano, L. C. (2018). The Late Triassic record of cynodonts: Time of innovations in the mammalian lineage. In L. H. Tanner (Ed.), *The Late Triassic world: Earth in a time of transition* (pp. 407–445). Springer International Publishing, Topics in geobiology. https://doi.org/10.1007/978-3-319-68009-5_11

Abdala, F., Gaetano, L. C., Martinelli, A. G., Soares, M. B., Hancox, P. J., & Rubidge, B. S. (2020). Non-mammaliaform cynodonts from western Gondwana and the significance of Argentinean forms in enhancing understanding of the group. *Journal of South American Earth Sciences*, *104*, 102884. https://doi.org/10.1016/j.jsames.2020.102884

Abdala, F., Gaetano, L. C., Smith, R. M. H., & Rubidge, B. S. (2019). A new large cynodont from the Late Permian (Lopingian) of the South African Karoo Basin and its phylogenetic significance. *Zoological Journal of the Linnean Society*, *186*, 983–1005. https://doi.org/10.1093/zoolinnean/zlz004

Abdala, F., Neveling, J., & Welman, J. (2006). A new trirachodontid cynodont from the lower levels of the Burgersdorp Formation (Lower Triassic) of the Beaufort Group, South Africa and the cladistic relationships of Gondwanan gomphodonts. *Zoological Journal of the Linnean Society*, *147*, 383–413. https://doi.org/10.1111/j.1096-3642.2006.00224.x

Abdala, F., & Ribeiro, A. M. (2003). A new traversodontid cynodont from the Santa Maria Formation (Ladinian-Carnian) of southern Brazil, with a phylogenetic analysis of Gondwanan traversodontids. *Zoological Journal of the Linnean Society*, *139*, 529–545. https://doi.org/10.1111/j.1096-3642.2003.00096.x

Abdala, F., & Ribeiro, A. M. (2010). Distribution and diversity patterns of Triassic cynodonts (Therapsida, Cynodontia) in Gondwana. *Palaeogeography, Palaeoclimatology, Palaeoecology*, *286*, 202–217. https://doi.org/10.1016/j.palaeo.2010.01.011

Abdala, F., & Sa-Teixeira, A. M. (2004). A traversodontid cynodont of African affinity in the South American Triassic. *Palaeontologia Africana*, *40*, 11–22.

Adams, D. C., & Otárola-Castillo, E. (2013). geomorph: An r package for the collection and analysis of geometric morphometric shape data. *Methods in Ecology and Evolution*, *4*, 393–399. https://doi.org/10.1111/2041-210X.12035

Araújo, R., David, R., Benoit, J., Lungmus, J. K., Stoessel, A., Barrett, P. M., Maisano, J. A., Ekdale, E., Orliac, M., Luo, Z.-X., Martinelli, A. G., Hoffman, E. A., Sidor, C. A., Martins, R. M. S., Spoor, F., & Angielczyk, K. D. (2022). Inner ear biomechanics reveals a Late Triassic origin for mammalian endothermy. *Nature*, *607*, 726–731. https://doi.org/10.1038/s41586-022-04963-z

19328494, 2024, 4, Downloaded from https://anatomypubs.onlinelibrary.wiley.com/doi/10.1002/ar.25386 by University Of Witwatersrand, Wiley Online Library on [07/11/2024]. See the Terms and Conditions (https://onlinelibrary.wiley.com/terms-and-conditions) on Wiley Online Library for rules of use; OA articles are governed by the applicable Creative Commons License

Barrett, P. M., & Upchurch, P. (2005). Sauropodomorph diversity through time. In K. A. Currie Rogers & J. A. Wilson (Eds.), *The Sauropods: Evolution and Paleobiology*, (pp. 125–156). University of California Press.

Benavente, C. A., Mancuso, A. C., Irmis, R. B., Bohacs, K. M., & Matheos, S. (2021). Tectonically conditioned record of continental interior paleoclimate during the Carnian Pluvial Episode: The Upper Triassic Los Rastros Formation, Argentina. *GSA Bulletin*, *134*, 60–80. https://doi.org/10.1130/B35847.1

Boivin, M., Álvarez, A., & Ercoli, M. D. (2022). Integration patterns of cheek teeth and ecomorphological evolution in grinding herbivores: The case of caviine rodents (Caviomorpha: Caviidae). *Zoological Journal of the Linnean Society*, *196*, 1094–1116. https://doi.org/10.1093/zoolinnean/zlac005

Boivin, M., & Marivaux, L. (2020). Dental homologies and evolutionary transformations in Caviomorpha (Hystricognathi, Rodentia): New data from the Paleogene of Peruvian Amazonia. *Historical Biology*, *32*, 528–554. https://doi.org/10.1080/08912963.2018.1506778

Bomfleur, B., Blomenkemper, P., Kerp, H., & McLoughlin, S. (2018). Chapter 24—Polar regions of the Mesozoic–Paleogene greenhouse world as refugia for relict plant groups. In M. Krings, C. J. Harper, N. R. Cúneo, & G. W. Rothwell (Eds.), (pp. 593–611). Academic Press. https://doi.org/10.1016/B978-0-12-813012-4.00024-3

Bonaparte, J. F. (1962). Descripcion del craneo y mandibula de *Exaeretodon frenguellii* Cabrera y su comparacion con Diademodontidae, Tritylodontidae y los cinodontes sudamericanos. *Publicaciones del Museo Municipal de Ciencias Naturales y Tradicionales de Mar del Plata*, *1*, 135–202.

Brink, A. S. (1963). Two cynodonts from the Ntawere Formation in the Luangwa valley of Northern Rhodesia. *Palaeontologia Africana*, *8*, 77–96.

Cariglino, B., Monti, M., & Zavattieri, A. M. (2018). A Middle Triassic macroflora from southwestern Gondwana (Mendoza, Argentina) with typical Northern Hemisphere elements: Biostratigraphic, palaeogeographic and palaeoenvironmental implications. *Review of Palaeobotany and Palynology*, *257*, 1–18. https://doi.org/10.1016/j.revpalbo.2018.06.004

Cariglino, B., Zavattieri, A. M., Gutiérrez, P. R., & Balarino, M. L. (2016). The paleobotanical record of the Triassic Cerro de Las Cabras Formation at its type locality, Potrerillos, Mendoza (Uspallata Group): An historical account and first reccord of fossil flora. *Ameghiniana*, *53*, 184–204. https://doi.org/10.5710/AMGH.17.12.2015.2952

Christensen, K., & Melstrom, K. M. (2021). Quantitative analyses of squamate dentition demonstrate novel morphological patterns. *PLoS One*, *16*, e0257427. https://doi.org/10.1371/journal.pone.0257427

Cignoni, P., Callieri, M., Corsini, M., Dellepiane, M., Ganovelli, F., & Ranzuglia, G. (2008). MeshLab: An open-source mesh processing tool. In V. Scarano, R. D. Chiara, & U. Erra (Eds.), *Eurographics Italian Chapter Conference* (pp. 129–136). The Eurographics Association. https://doi.org/10.2312/LocalChapterEvents/ItalChap/ItalianChapConf2008/129-136

Cignoni, P., & Ranzuglia, G. (2014). MeshLab: An open-source mesh processing tool. MeshLab Visual Computing Lab—IST-CNR. https://www.meshlab.sourceforge.net/

Cohen, K. M., Harper, D. A. T., & Gibbard, P. L. (2023). ICS international chronostratigraphic chart 2023/06. *International Commission on Stratigraphy, IUGS*. www.stratigraphy.org (visited: 2023/07/12)

Crompton, A., & Attridge, J. (1986). Masticatory apparatus of the larger herbivores during Late Triassic and Early Jurassic times. In K. Padian (Ed.), *The beginning of the age of dinosaurs: Faunal change across the Triassic-Jurassic boundary* (pp. 223–236). Cambridge University Press.

Crompton, A. W. (1972). Postcanine occlusion in cynodonts and tritylodontids. *Bulletin of the British Museum (Natural History) (Geology)*, *21*, 29–71.

Crompton, A. W., & Jenkins, F. A. (1968). Molar occlusion in Late Triassic mammals. *Biological Reviews*, *43*, 427–458. https://doi.org/10.1111/j.1469-185X.1968.tb00966.x

Donnadieu, Y., Pierrehumbert, R., Jacob, R., & Fluteau, F. (2006). Modelling the primary control of paleogeography on Cretaceous climate. *Earth and Planetary Science Letters*, *248*, 426–437. https://doi.org/10.1016/j.epsl.2006.06.007

Evans, A. R., Wilson, G. P., Fortelius, M., & Jernvall, J. (2007). High-level similarity of dentitions in carnivorans and rodents. *Nature*, *445*, 78–81. https://doi.org/10.1038/nature05433

Filippini, F. S., Abdala, F., & Cassini, G. H. (2022). Body mass estimation in Triassic cynodonts from Argentina based on limb variables. *Acta Palaeontologica Polonica*, *67*, 543–557.

Flynn, J. J., Parrish, J. M., Rakotosamimanana, B., Ranivoharimanana, L., Simpson, W. F., & Wyss, A. R. (2000). New traversodontids (Synapsida: Eucynodontia) from the Triassic of Madagascar. *Journal of Vertebrate Paleontology*, *20*, 422–427. https://doi.org/10.1671/0272-4634(2000)020[0422:NTSEFT]2.0.CO;2

Gaetano, L. C., Abdala, F., Seoane, F. D., Tartaglione, A., Schulz, M., Otero, A., Leardi, J. M., Apaldetti, C., Krapovickas, V., & Steimbach, E. (2022). A new cynodont from the Upper Triassic Los Colorados Formation (Argentina, South America) reveals a novel paleobiogeographic context for mammalian ancestors. *Scientific Reports*, *12*, 6451. https://doi.org/10.1038/s41598-022-10486-4

Gao, K.-Q., Fox, R. C., Zhou, C.-F., & Li, D.-Q. (2010). A new non-mammalian eucynodont (Synapsida: Therapsida) from the Triassic of Northern Gansu Province, China, and its biostratigraphic and biogeographic implications. *American Museum Novitates*, *3685*, 1–25. https://doi.org/10.1206/649.1

Godefroit, P. (1999). New traversodontid (Therapsida: Cynodontia) teeth from the Upper Triassic of Habay-la-Vieille (Southern Belgium). *Paläontologische Zeitschrift*, *73*, 385–394. https://doi.org/10.1007/BF02988049

Godefroit, P., & Battail, B. (1997). Late Triassic cynodonts from Saint-Nicolas-de-Port (north-eastern France). *Geodiversitas*, *19*, 567–631.

Goñi, R. G., & Goin, F. J. (1988). Morfología dentaria y biomecánica masticatoria de los cinodontes (Reptilia, Therapsida) del Triásico Argentino; I, *Andescynodon mendozensis* Bonaparte (Traversodontidae). *Ameghiniana*, *25*, 139–148.

Goñi, R. G., & Goin, F. J. (1991). Morfología dentaria y biomecánica masticatoria de los cinodontes (Reptilia, Therapsida) del Triásico argentino: II. *Exaeretodon frenguellii* Cabrera (Traversodontidae). *Ameghiniana*, *27*, 327–336.

Goswami, A., Flynn, J. J., Ranivoharimanana, L., & Wyss, A. R. (2005). Dental microwear in Triassic amniotes: Implications for paleoecology and masticatory mechanics. *Journal of Vertebrate*

19328494, 2024, 4, Downloaded from https://anatomypubs.onlinelibrary.wiley.com/doi/10.1002/ar.25386 by University Of Witwatersrand, Wiley Online Library on [07/11/2024]. See the Terms and Conditions (https://onlinelibrary.wiley.com/terms-and-conditions) on Wiley Online Library for rules of use; OA articles are governed by the applicable Creative Commons License

Paleontology, *25*, 320–329. https://doi.org/10.1671/0272-4634(2005)025[0320:DMITAI]2.0.CO;2

Gow, C. E. (1978). The advent of herbivory in certain reptilian lineages during the Triassic. *Palaeontologia Africana*, *21*, 133–141.

Hahn, G., Lepage, J.-C., & Wouters, G. (1988). Traversodontiden-Zähne (Cynodontia) aus der ober-Trias von Gaume (Süd-Belgien). *Bulletin-Institut Royal des Sciences Naturelles de Belgique. Sciences de la Terre*, *58*, 177–186.

Hendrickx, C., Abdala, F., & Choiniere, J. (2016). Postcanine microstructure in *Cricodon metabolus*, a Middle Triassic gomphodont cynodont from south-eastern Africa. *Palaeontology*, *59*, 851–861. https://doi.org/10.1111/pala.12263

Hendrickx, C., Abdala, F., & Choiniere, J. N. (2019). A proposed terminology for the dentition of gomphodont cynodonts and dental morphology in Diademodontidae and Trirachodontidae. *PeerJ*, *7*, 1–71. https://doi.org/10.7717/peerj.6752

Hendrickx, C., Gaetano, L. C., Choiniere, J. N., Mocke, H., & Abdala, F. (2020). A new traversodontid cynodont with a peculiar postcanine dentition from the Middle/Late Triassic of Namibia and dental evolution in basal gomphodonts. *Journal of Systematic Palaeontology*, *18*, 1669–1706. https://doi.org/10.1080/14772019.2020.1804470

Hendrickx, C., Mateus, O., & Araújo, R. (2015). A proposed terminology of theropod teeth (Dinosauria, Saurischia). *Journal of Vertebrate Paleontology*, *35*, e982797. https://doi.org/10.1080/02724634.2015.982797

Hillson, S. (2005). *Teeth* (2nd ed., p. 373). Cambridge University Press.

Hopson, J. A. (1985). Morphology and relationships of *Gomphodontosuchus brasiliensis* von Huene (Synapsida, Cynodontia, Tritylodontoidea) from the Triassic of Brazil. *Neues Jahrbuch für Geologie und Paläontologie, Monatshefte*, *1985*, 285–299.

Hopson, J. A. (2005). A juvenile gomphodont cynodont specimen from the *Cynognathus* Assemblage Zone of South Africa: Implications for the origin of gomphodont postcanine morphology. *Palaeontologia Africana*, *41*, 53–66.

Hopson, J. A. (2014). The traversodontid cynodont *Mandagomphodon hirschsoni* from the Middle Triassic of the Ruhuhu Valley, Tanzania. In C. F. Kammerer, K. D. Angielczyk, & J. Fröbisch (Eds.), *Early evolutionary history of the Synapsida* (pp. 233–253). Springer Netherlands, Dordrecht, Vertebrate paleobiology and paleoanthropology. https://doi.org/10.1007/978-94-007-6841-3_14

Hopson, J. A., & Barghusen, H. R. (1986). An analysis of therapsid relationships. In N. Hotton, III, P. D. MacLean, J. J. Roth, & E. C. Roth (Eds.), *The ecology and biology of mammal-like reptiles* (pp. 83–106). Smithsonian Institution Press.

Hopson, J. A., & Kitching, J. W. (1972). A revised classification of cynodonts (Reptilia; Therapsida). *Palaeontologia Africana*, *14*, 71–75.

Hopson, J. A., & Kitching, J. W. (2001). A probainognathian cynodont from South Africa and the phylogeny of nonmammalian cynodonts. *Bulletin of the Museum of Comparative Zoology*, *156*, 5–35.

Huttenlocker, A. K., & Sidor, C. A. (2020). A basal nonmammaliaform cynodont from the Permian of Zambia and the origins of mammalian endocranial and postcranial anatomy. *Journal of Vertebrate Paleontology*, *40*, e1827413. https://doi.org/10.1080/02724634.2020.1827413

Kammerer, C. F. (2016). A new taxon of cynodont from the *Tropidostoma* Assemblage Zone (upper Permian) of South Africa, and the early evolution of Cynodontia. *Papers in Palaeontology*, *2*, 387–397.

Kammerer, C. F., Flynn, J. J., Ranivoharimanana, L., & Wyss, A. R. (2008). New material of *Menadon besairiei* (Cynodontia: Traversodontidae) from the Triassic of Madagascar. *Journal of Vertebrate Paleontology*, *28*, 445–462. https://doi.org/10.1671/0272-4634(2008)28[445:NMOMBC]2.0.CO;2

Kemp, T. S. (1980). Aspects of the structure and functional anatomy of the Middle Triassic cynodont *Luangwa*. *Journal of Zoology*, *191*, 193–239.

Kemp, T. S. (2005). *The origin and evolution of mammals* (1st ed., p. 342). Oxford University Press.

Kubo, T., Yamada, E., & Kubo, M. O. (2017). Masticatory jaw movement of *Exaeretodon argentinus* (Therapsida: Cynodontia) inferred from its dental microwear. *PLoS One*, *12*, e0188023. https://doi.org/10.1371/journal.pone.0188023

Kustatscher, E., Ash, S. R., Karasev, E., Pott, C., Vajda, V., Yu, J., & McLoughlin, S. (2018). Flora of the Late Triassic. In L. H. Tanner (Ed.), *The Late Triassic world: Earth in a time of transition* (pp. 545–622). Springer International Publishing, Topics in geobiology. https://doi.org/10.1007/978-3-319-68009-5_13

Lane, A., Janis, C. M., & Sepkoski, J. J. (2005). Estimating paleodiversities: A test of the taxic and phylogenetic methods. *Paleobiology*, *31*, 21–34. https://doi.org/10.1666/0094-8373(2005)031<0021:EPATOT>2.0.CO;2

Liparini, A., Oliveira, T. V., Pretto, F. A., Soares, M. B., & Schultz, C. L. (2013). The lower jaw and dentition of the traversodontid *Exaeretodon riograndensis* Abdala, Barberena & Dornelles, from the Brazilian Triassic (Santa Maria 2 Sequence, *Hyperodapedon* Assemblage Zone). *Alcheringa: An Australasian Journal of Palaeontology*, *37*, 331–337. https://doi.org/10.1080/03115518.2013.752607

Liu, J., & Abdala, F. (2014). Phylogeny and taxonomy of the Traversodontidae. In C. F. Kammerer, K. D. Angielczyk, & J. Fröbisch (Eds.), *Early evolutionary history of the Synapsida* (pp. 255–279). Springer Netherlands, Vertebrate paleobiology and paleoanthropology. https://doi.org/10.1007/978-94-007-6841-3_15

Liu, J., & Olsen, P. (2010). The phylogenetic relationships of Eucynodontia (Amniota: Synapsida). *Journal of Mammalian Evolution*, *17*, 151–176. https://doi.org/10.1007/s10914-010-9136-8

Liu, J., & Sues, H.-D. (2010). Dentition and tooth replacement of *Boreogomphodon* (Cynodontia: Traversodontidae) from the Upper Triassic of North Carolina, USA. *Vertebrata PalAsiatica*, *48*, 169–184.

Mancuso, A. C., Benavente, C. A., Irmis, R. B., & Mundil, R. (2020). Evidence for the Carnian Pluvial Episode in Gondwana: New multiproxy climate records and their bearing on early dinosaur diversification. *Gondwana Research*, *86*, 104–125. https://doi.org/10.1016/j.gr.2020.05.009

Mancuso, A. C., Horn, B. L. D., Benavente, C. A., Schultz, C. L., & Irmis, R. B. (2021). The paleoclimatic context for South American Triassic vertebrate evolution. *Journal of South American Earth Sciences*, *110*, 103321. https://doi.org/10.1016/j.jsames.2021.103321

Martinelli, A. G. (2010). On the postcanine dentition of *Pascualgnathus polanskii* Bonaparte (Cynodontia, Traversodontidae) from the Middle Triassic of Argentina. *Geobios*, *43*, 629–638. https://doi.org/10.1016/j.geobios.2010.03.006

Martinelli, A. G., Kammerer, C. F., Melo, T. P., Neto, V. D. P., Ribeiro, A. M., Da-Rosa, Á. A., Schultz, C. L., & Soares, M. B.

19328494, 2024, 4, Downloaded from https://anatomypubs.onlinelibrary.wiley.com/doi/10.1002/ar.25386 by University Of Witwatersrand, Wiley Online Library on [07/11/2024]. See the Terms and Conditions (https://onlinelibrary.wiley.com/terms-and-conditions) on Wiley Online Library for rules of use; OA articles are governed by the applicable Creative Commons License

(2017). The African cynodont *Aleodon* (Cynodontia, Probainognathia) in the Triassic of southern Brazil and its biostratigraphic significance. *PLoS One*, *12*, e0177948.

Melo, T. P., Abdala, F., & Soares, M. B. (2015). The Malagasy cynodont *Menadon besairiei* (Cynodontia; Traversodontidae) in the Middle–Upper Triassic of Brazil. *Journal of Vertebrate Paleontology*, *35*, e1002562. https://doi.org/10.1080/02724634.2014.1002562

Melo, T. P., Martinelli, A. G., & Soares, M. B. (2017). A new gomphodont cynodont (Traversodontidae) from the Middle–Late Triassic *Dinodontosaurus* Assemblage Zone of the Santa Maria Supersequence, Brazil. *Palaeontology*, *60*, 571–582. https://doi.org/10.1111/pala.12302

Melo, T. P., Ribeiro, A. M., Martinelli, A. G., & Soares, M. B. (2019). Early evidence of molariform hypsodonty in a Triassic stem-mammal. *Nature Communications*, *10*, 2841. https://doi.org/10.1038/s41467-019-10719-7

Melstrom, K. M. (2017). The relationship between diet and tooth complexity in living dentigerous saurians. *Journal of Morphology*, *278*, 500–522. https://doi.org/10.1002/jmor.20645

Melstrom, K. M., Chiappe, L. M., & Smith, N. D. (2021). Exceptionally simple, rapidly replaced teeth in sauropod dinosaurs demonstrate a novel evolutionary strategy for herbivory in Late Jurassic ecosystems. *BMC Ecology and Evolution*, *21*, 202. https://doi.org/10.1186/s12862-021-01932-4

Melstrom, K. M., & Irmis, R. B. (2019). Repeated evolution of herbivorous crocodyliforms during the age of dinosaurs. *Current Biology*, *29*, 2389–2395.e3. https://doi.org/10.1016/j.cub.2019.05.076

Miron, L. R., Pavanatto, A. E. B., Pretto, F. A., Müller, R. T., Dias-da-Silva, S., & Kerber, L. (2020). *Siriusgnathus niemeyerorum* (Eucynodontia: Gomphodontia): The youngest South American traversodontid? *Journal of South American Earth Sciences*, *97*, 102394. https://doi.org/10.1016/j.jsames.2019.102394

Pampush, J. D., Winchester, J. M., Morse, P. E., Vining, A. Q., Boyer, D. M., & Kay, R. F. (2016). Introducing molaR: A new R package for quantitative topographic analysis of teeth (and other topographic surfaces). *Journal of Mammalian Evolution*, *23*, 397–412. https://doi.org/10.1007/s10914-016-9326-0

Pavanatto, A. E. B., Pretto, F. A., Kerber, L., Müller, R. T., Da-Rosa, Á. A. S., & Dias-da-Silva, S. (2018). A new Upper Triassic cynodont-bearing fossiliferous site from southern Brazil, with taphonomic remarks and description of a new traversodontid taxon. *Journal of South American Earth Sciences*, *88*, 179–196. https://doi.org/10.1016/j.jsames.2018.08.016

Pineda-Munoz, S., Evans, A. R., & Alroy, J. (2016). The relationship between diet and body mass in terrestrial mammals. *Paleobiology*, *42*, 659–669. https://doi.org/10.1017/pab.2016.6

Ranivoharimanana, L., Kammerer, C. F., Flynn, J. J., & Wyss, A. R. (2011). New material of *Dadadon isaloi* (Cynodontia, Traversodontidae) from the Triassic of Madagascar. *Journal of Vertebrate Paleontology*, *31*, 1292–1302. https://doi.org/10.1080/039.031.0619

Rayner, R. R., Butler, R. J., Kammerer, C. F., & Choiniere, J. N. (2022). *Guttigomphus avilionis* gen. et sp. nov., a trirachodontid cynodont from the upper *Cynognathus* Assemblage Zone, Burgersdorp Formation of South Africa. *PeerJ*, *10*, e14355. https://doi.org/10.7717/peerj.14355

Reichel, M., Schultz, C. L., & Soares, M. B. (2009). A new traversodontid cynodont (Therapsida, Eucynodontia) from the Middle Triassic Santa Maria Formation of Rio Grande Do Sul, Brazil. *Palaeontology*, *52*, 229–250. https://doi.org/10.1111/j.1475-4983.2008.00824.x

Reisz, R. R., & Sues, H.-D. (2000). Herbivory in late Paleozoic and Triassic terrestrial vertebrates. In H.-D. Sues (Ed.), *Evolution of herbivory in terrestrial vertebrates* (pp. 9–41). Cambridge University Press.

Romer, A. S. (1967). The Chañares (Argentina) Triassic reptile fauna. III. Two new gomphodonts, *Massetognathus pascuali* and *M. teruggii*. *Breviora*, *264*, 1–25.

Ruta, M., Botha-Brink, J., Mitchell, S. A., & Benton, M. J. (2013). The radiation of cynodonts and the ground plan of mammalian morphological diversity. *Proceedings of the Royal Society of London B: Biological Sciences*, *280*, 20131865. https://doi.org/10.1098/rspb.2013.1865

Santana, S. E., Strait, S., & Dumont, E. R. (2011). The better to eat you with: Functional correlates of tooth structure in bats. *Functional Ecology*, *25*, 839–847. https://doi.org/10.1111/j.1365-2435.2011.01832.x

Schmitt, M. R., Martinelli, A. G., Kaiuca, J. F. L., Schultz, C. L., & Soares, M. B. (2024). Old fossil findings in the Upper Triassic rocks of southern Brazil improve diversity of traversodontid cynodonts (Therapsida, Cynodontia). *The Anatomical Record*, *307*(4), 1474–1514. https://doi.org/10.1002/ar.25244

Schwenk, K. (2000). *Feeding: Form, function and evolution in tetrapod vertebrates* (p. 556). Academic Press.

Seeley, H. G. (1895). Researches on the structure, organization, and classification of the fossil Reptilia. Part IX., section 4. On the Gomphodontia. *Philosophical Transactions of the Royal Society of London B*, *186*, 1–57.

Seeley, H. G. (1908). Additional evidence as to the dentition and structure of the skull in the South African fossil reptile genus *Diademodon*. *Proceedings of the Zoological Society of London*, *78*, 611–617. https://doi.org/10.1111/j.1469-7998.1908.tb07394.x

Sidor, C. A., & Hopson, J. A. (2018). *Cricodon metabolus* (Cynodontia: Gomphodontia) from the Triassic Ntawere Formation of northeastern Zambia: Patterns of tooth replacement and a systematic review of the Trirachodontidae. In: C. A. Sidor, & S. J. Nesbitt, (Eds.), *Vertebrate and climatic evolution in the Triassic rift basins of Tanzania and Zambia*. Society of Vertebrate Paleontology Memoir 17. Journal of Vertebrate Paleontology, 37(6, Supplement), 39–64.

Smith, J. B., & Dodson, P. (2003). A proposal for a standard terminology of anatomical notation and orientation in fossil vertebrate dentitions. *Journal of Vertebrate Paleontology*, *23*, 1–12. https://doi.org/10.1671/0272-4634(2003)23[1:APFAST]2.0.CO;2

Spalletti, L. A., Artabe, A. E., & Morel, E. M. (2003). Geological factors and evolution of southwestern Gondwana Triassic plants. *Gondwana Research*, *6*, 119–134. https://doi.org/10.1016/S1342-937X(05)70648-1

Ungar, P. S. (2010). *Mammal teeth: Origin, evolution, and diversity* (p. 320). Johns Hopkins University Press.

Velazco, P. M., Buczek, A. J., & Novacek, M. J. (2017). Two new tritylodontids (Synapsida, Cynodontia, Mammaliamorpha) from the Upper Jurassic, southwestern Mongolia. *American Museum Novitates*, *2017*, 1–35.

19328494, 2024, 4, Downloaded from https://anatomypubs.onlinelibrary.wiley.com/doi/10.1002/ar.25386 by University Of Witwatersrand, Wiley Online Library on [07/11/2024]. See the Terms and Conditions (https://onlinelibrary.wiley.com/terms-and-conditions) on Wiley Online Library for rules of use; OA articles are governed by the applicable Creative Commons License

Wilson, G. P., Evans, A. R., Corfe, I. J., Smits, P. D., Fortelius, M., & Jernvall, J. (2012). Adaptive radiation of multituberculate mammals before the extinction of dinosaurs. *Nature*, *483*, 457–460. https://doi.org/10.1038/nature10880

Winchester, J. M. (2016). MorphoTester: An open source application for morphological topographic analysis. *PLoS One*, *11*, e0147649. https://doi.org/10.1371/journal.pone.0147649

Wynd, B., Abdala, F., & Nesbitt, S. J. (2022). Ontogenetic growth in the crania of *Exaeretodon argentinus* (Synapsida: Cynodontia) captures a dietary shift. *PeerJ*, *10*, e14196. https://doi.org/10.7717/peerj.14196

Young, C. (1959). Note on the first cynodont from the *Sinokannemeyeria* faunas in Shansi, China. *Vertebrata PalAsiatica*, *3*, 124–132.

SUPPORTING INFORMATION

Additional supporting information can be found online in the Supporting Information section at the end of this article.

How to cite this article: Hendrickx, C., Abdala, F., Filippini, F. S., Wills, S., Benson, R., & Choiniere, J. N. (2024). Evolution of postcanine complexity in Gomphodontia (Therapsida: Cynodontia). *The Anatomical Record*, *307*(4), 1613–1633. https://doi.org/10.1002/ar.25386

19328494, 2024, 4, Downloaded from https://anatomypubs.onlinelibrary.wiley.com/doi/10.1002/ar.25386 by University Of Witwatersrand, Wiley Online Library on [07/11/2024]. See the Terms and Conditions (https://onlinelibrary.wiley.com/terms-and-conditions) on Wiley Online Library for rules of use; OA articles are governed by the applicable Creative Commons License